Investigating the Relationship Between Cystic Fibrosis Transmembrane Conductance Regulator and Colorectal Cancer Under Endoplasmic Reticulum Stress

A Thesis SUBMITTED TO THE FACULTY OF

UNIVERSITY OF MINNESOTA

BY

Zishan Zhang

IN PARTIAL FULFILLMENT OF THE REQUIREMENTS

FOR THE DEGREE OF

MASTER OF SCIENCE

Dr. Patricia Scott, Dr. Robert Cormier

April 2018

Acknowledgements

First and foremost, I would like to express my sincere gratitude to my advisors, Dr. Patricia Scott and Dr. Robert Cormier, for their continuous support of my graduate study and research, for their patience, motivation, enthusiasm, and immense knowledge. Their guidance helped me in completing the research and writing of this thesis. I could not have imagined having better advisors and mentors for my graduate studies.

I gratefully acknowledge my committee member Dr. Lynne Bemis for her instructions and encouragement throughout my graduate career.

I also would like to thank my lab members: Kyle Anderson, Rebecca Madden, Mekhla Singhania, and Amanda Palme for their friendship and help. Kyle Anderson taught me a lot and gave me insightful comments. Amanda Palme contributed to this work greatly.

My special thanks go to our collaborators at the University of Minnesota Twin Cities, David Largaespada, Tim Starr, our collaborators at Case Western Reserve University, Mitchell Drumm, Craig Hodges, and our collaborator at the Netherlands Cancer Institute, Amsterdam- Janneke Linnekamp.

Finally, I want to thank the Integrated Biosciences Graduate Program, National Cancer Institute, Whiteside Institute for Clinical Research, Randy Shaver Cancer Research and Community Fund, and the Mezin- Koats Colon Cancer Research for providing the financial support for this study.

Dedication

This thesis work is dedicated to my parents who have been a constant source of support and encouragement during the challenges of graduate school and life. I am truly thankful for having you in my life. You have always loved me unconditionally, and your good examples have taught me to work hard for the things that I aspire to achieve.

Abstract

Our group has identified Cystic Fibrosis Transmembrane Conductance Regulator (*CFTR*) as a tumor suppressor for colorectal cancer (CRC) (Than *et al*., 2016). However, the mechanism by which *CFTR* protects against CRC is unknown. Determining this mechanism may lead to new therapies for CRC. Gene Set Enrichment Analysis (GSEA) pathway analysis showed that *CFTR*-deficient normal and tumor tissues from mice and humans were enriched in genes involved in the unfolded protein response (UPR) to endoplasmic reticulum (ER) stress. Altered genes, environmental stress and increased protein synthesis induce UPR activation in cancer cells (Kaufman & Wang, 2014; Ma & Hendershot, 2004; Dejeans, Barroso, Fernandez-Zapico, Samali, Chevet, 2015). The UPR has two potentially opposing effects on cancer development: on the one hand, some cancer cells require a higher level of UPR to support their growth and survival (Corazzari, Gagliardi, Fimia & Piacentini, 2017); on the other hand, increased UPR leads to loss of stemness which could inhibit cancer development (Heijmans *et al*., 2013). To identify the correlation between UPR and cancer-supporting effects of *CFTR*-deficiency, a pair of *CFTR* knockout (KO) and wildtype (WT) Caco2 cell lines created by CRISPR-Cas9 engineering were utilized to test the working model that UPR activation might be enhanced in *CFTR* KO cells, and this activation might support CRC cell survival under ER stress. To test the working model, the Caco2 cell lines were treated with chemical inducers to trigger ER stress. To evaluate the UPR activities, we used Thapsigargin (TG) to induce ER stress in *CFTR* KO and WT cell lines and compared

mRNA expression changes of key genes in the two cell lines by performing RT-qPCR. The heat shock protein A member 5 (*HSPA5)* gene encodes the protein that initiates all three UPR sub-pathways. Although the expression of *HSPA5* increased after TG treatment in both *CFTR* WT and *CFTR* KO cell lines, the TG treatment had more of an effect on *HSPA5* expression in *CFTR* KO cells, suggesting a trend that CFTR deficiency might enhance the effect of ER stress on the expression of UPR gatekeeper *HSPA5,* the common regulator for initiating three UPR sub-pathways. The *ATF4* expression levels in both *CFTR* WT and *CFTR* KO cell lines increased to the same extent, which reflects that the loss of *CFTR* might not promote the activation of PERK signaling. The decreased total *XBP1* mRNA expression levels in *CFTR* KO cells suggests that *CFTR* deficiency might not activate the specific IRE1α-XBP1 signaling pathway. The *TXNIP*, which is part of an apoptotic pathway, is down-regulated in *CFTR* KO cells, which might provide protection from apoptosis. These studies suggest that UPR activation might be enhanced in *CFTR* KO cells, but the specific pathway might not be the one detected. Additionally, the down regulation of *TXNIP* might offer protection for CRC cells from apoptosis.

Although many cancer cells require an enhanced UPR (Corazzari, Gagliardi, Fimia & Piacentini, 2017), excessive, prolonged activation triggers a switch to an apoptotic pathway (Wang & Kaufman, 2016; Niederreiter, L. *et al.,* 2013). To examine this possibility, TG and Tunicamycin (TM) were used to induce ER stress in cells, and cell viability in *CFTR* KO and WT cell lines over time was compared by conducting MTT assay. Although the results showed decreased cell viability after treatment in both

CFTR WT and *CFTR* KO cell lines, the ratios of treated over untreated viability at each point after TG and TM treatment was higher in *CFTR* KO cells, indicating that the loss of CFTR might cause TG-induced ER stress to have less of an effect on cell viability. These data suggest that the loss of *CFTR* increases protection from ER stress, and that this protection supports the survival of CRC cells.

Based on the fact that *CFTR* deficiency can activate the NF-κB signaling pathway (Crites *et al*., 2015), and that UPR can activate the NF-κB (Grootjans, Kaser, Kaufman & Blumberg, 2016), the NF-κB activity in *CFTR* KO cells in response to UPR was also examined. RT-qPCR analysis was performed to compare the gene expression changes relating to NF-κB signaling pathway in *CFTR* WT and *CFTR* KO Caco2 cell lines treated with TG to trigger UPR activation. Although the results showed enhanced expression of *IL8* and *TNF* in both cell lines, the TG treatment had less of an effect on the expression of these genes in *CFTR* KO cells. This suggests that *CFTR* deficiency might cause TG to produce less of an effect on the expression of NF-κB signaling target genes *IL8* and *TNF*. These data suggest that the loss of *CFTR* might cause TG-induced UPR to have less of an effect on NF-κB activation. The enhanced basal expression levels of the NF-κB target gene *IL8* in *CFTR* KO cells might suggest an increased activation of NF-κB signaling in *CFTR* KO cells and this activation might support the growth of cancer cells.

In conclusion, in Caco2 CRC cells, *CFTR* deficiency may alter the response to UPR in several pathways, which may promote cancer cell survival. Additional experiments

must be conducted to determine which pathways among those that are altered are vital for cancer development.

Table of Contents

List of Figures

Introduction

Colorectal Cancer

Colorectal cancer (CRC) is the third leading cause of cancer deaths all over the world (Rosa *et al.*, 2015). It is estimated that in 2018, about 50,630 people will die of colorectal cancer in the US (The American Cancer Society, 2018). Colorectal cancer starts in the large intestine or rectum (Heath, 2010). If you observe a cross section of a colon from the inside out, the layer closet to the lumen is called the mucosa, which is composed of epithelium, lamina propria, and muscularis mucosae (Figure 1; Heath, 2010). The intestinal epithelium is structured as a simple columnar epithelium layer containing millions of "crypts of Lieberkuhn" that are goblet-shaped invaginations of the epithelium into the underlying connective tissue (Clevers, 2013; Heath, 2010). Benign tumors, or adenomas, start in epithelial cells and remain in the mucosal layer (Fearon *et al.*, 2011; Vogelstein, 1988). Adenomas can be detected through colonoscopy and surgically removed, and tumors cells will not likely grow back (Billings *et al.*, 2014; Zauber *et al.*, 2012). However, when tumor cells invade the submucosa layer, they form carcinomas (Fearon *et al.*, 2011; Vogelstein, 1988). These carcinomas are malignant and invade local and adjacent tissues (Fearon & Vogelstein, 1990). When malignant tumor cells travel to distant places in the body through the blood or the lymph system and form new tumors far from the original tumor, metastasis occurs (Martin, Ye, Sanders, Lane & Jiang, 2013). These metastatic cancer cells can damage important organs and cause death. In order to cure CRC, it is important to focus on its biology.

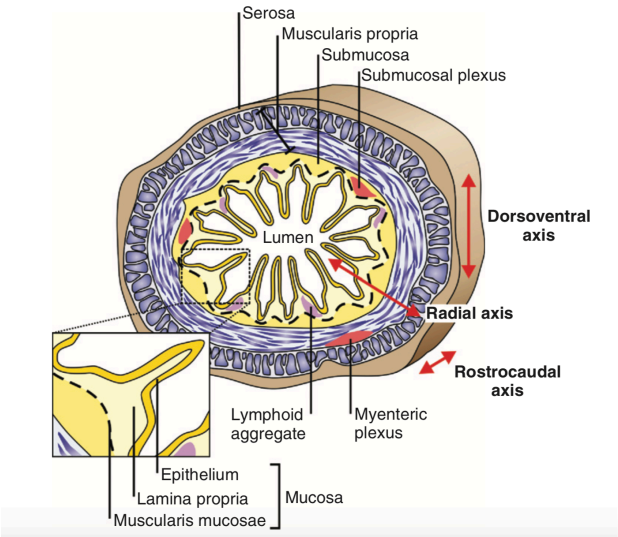

Figure 1. Organization of the intestine (Heath, 2010).

Intestinal Epithelial Cells

CRC starts in the intestinal epithelium, so concentrating on intestinal epithelial cells is necessary for the investigation into the biology of CRC. An intestinal stem cell generates a new stem cell and a transit-amplifying cell which cycles a limited number of times before differentiation (Clevers, 2013). The differentiated progeny cells include enterocytes, goblet cells, entero-endocrine cells, and Paneth cells (absent in the colon) (Clevers, 2013).

APC and Wnt/ β-catenin

Over 80% of colorectal cancer originates from mutations in a tumor suppressor gene called adenomatous polyposis coli (*APC*) (Brannon et al., 2014; Vogelstein & Kinzler, 1996). APC proteins control cell proliferation within the colon through regulating the conserved Wnt/β-Catenin pathway, which determines cell fate during

development (Clevers & Nusse, 2012). The APC protein resides in the destruction complex, together with the tumor suppressor proteins Axin and WTX and two constitutively active serine-threonine kinases (Li *et al*., 2012). The destruction complex phosphorylates and ubiquitinates β-catenin by β-TrCP, and β-catenin is degraded by a proteasome (Li *et al*., 2012; Clevers & Nusse, 2012). Intestinal stem cells located at the base of the crypt receive Wnt signals from stromal cells (Figure 2; Wetering *et al*., 2002). The binding of Wnts to the cell surface receptors saves the β-catenin from the degradation. The β-catenin migrates to the nucleus where it replaces the transcription repressor Groucho on TCF transcription factors to cause the transcription of Wnt target genes (Cavallo *et al*., 1998; Clevers & van der Flier, 2009). The β-catenin/TCF complex inhibits cell differentiation and maintains cell proliferation, which is important for maintaining the intestinal proliferative compartment (Wetering *et al*., 2002). Stem cell progenies move upward toward the lumen of the intestine and will not receive enough Wnt signals, leading to the degradation of β-catenin by a proteasome. The degradation of β-catenin will cause decreased cell proliferation and increased differentiation. When the APC protein is defective, the β-catenin will escape from the degradation, contributing to cell proliferation even in the absence of the Wnt signal. As a result, undifferentiated cells fail to move upward; instead they accumulate within the crypt and eventually form polyps.

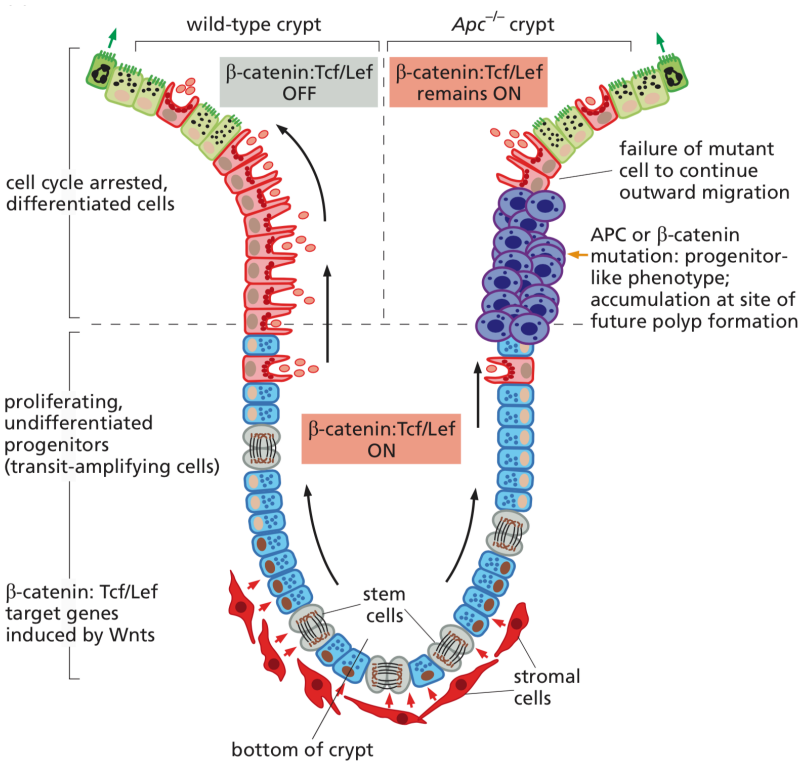

Figure 2. Model for the role of APC and Wnt/ β-catenin in the early stages of intestinal tumorigenesis (Wetering *et al*., 2002).

Cancer Stem Cells

It is believed that a minority of tumor cells, termed cancer stem cells (CSC), are responsible for tumor growth and spread (Khalek, Gallicano & Mishra, 2010). CSC are defined because they have characteristics similar to normal stem cells. They have self-renewal capacities that drive tumorgenesis and the property to aberrantly differentiate and generate the bulk of cells within a tumor (Khalek, Gallicano & Mishra, 2010). CRC is believed to initiate from the transformation of intestinal stem cells that have undergone oncogenic mutations. Leucine rich repeat containing G protein coupled receptor 5 (*Lgr5)* is an intestinal stem cell signature gene because it is expressed exclusively in the cycling columnar cells at the intestinal crypt base where intestinal

stem cells are located (Barker *et al.*, 2007). The *Lgr5*-positive crypt base columnar cells have the stem cell capacity to generate all intestinal epithelial lineages (Barker *et al.*, 2007). Stem cell-specific *Apc* deficiency induces intestinal adenoma in mice. *Apc* deficiency in *Lgr5*-positive crypt base columnar cells causes transformation of stem cells and maintenance at the crypt base to support the growth and development of adenoma in mice (Barker *et al.*, 2009).

Molecular Genetics of Colorectal Cancer

Mutations in *APC* lead to the accumulation of polyps or benign adenomas from which most colorectal cancers develop, but additional genetic alterations are required to cause invasive carcinomas (Fearon & Vogelstein, 1990; Clevers & van der Flier, 2009). Molecular alterations that allow the progression from adenomatous polyps to colorectal cancer might include the activation of oncogenes coupled with deficiencies of tumor suppressors. For example, the subsequent mutations in *p53*, *KRAS* and other genes that follow the formation of adenomas allow tumors to develop and become malignant and even metastatic (Dow *et al.*, 2015; Fearon & Vogelstein, 1990; Clevers & van der Flier, 2009). However, CRC is different in each patient. The accumulation of more than six gene mutations may be required to develop colorectal cancer (Calabrese *et al.*, 2005).

Desire for Identification of Other Drivers for Colorectal Cancer

To cure CRC, knowledge about mutations in main drivers, such as in APC, is currently insufficient. It is thus important to identify other genetic alterations required for CRC development. Understanding the full set of mutations in each patient's cancer and how these mutations affect the behavior of the cancer makes it possible for each

patient to receive precision medicine and better medical care. Not all of the altered genes in CRC patients are drivers for colorectal cancer. To identify genes that, when altered, would contribute to causing CRC, Sleeping Beauty (SB) transposon-based screens were conducted by Dr. Robert Cormier, Dr. David Largaespada and Dr. Timothy Starr at the University of Minnesota (Starr *et al.* 2009; Starr *et al.* 2011). These researchers introduced random insertional mutations in mice through a synthetic DNA transposon and then determined if these mutations caused intestinal tumors (Starr *et al.* 2009; Starr *et al.* 2011).

Cystic Fibrosis Transmembrane Conductance Regulator

Dr. Robert Cormier, Dr. David Largaespada and Dr. Timothy Starr identified 77 novel candidate genes for CRC, and 60 among these 77 candidate genes were dysreglated in human CRC (Starr *et al.* 2009). Among these 60 candidate drivers for human and murine CRC, the Cystic Fibrosis Transmembrane Conductance Regulator (*CFTR*) was determined to be a common insertion site candidate CRC gene in multiple SB transposon-based mutagenesis screens in mouse intestines (Starr *et al.,* 2009). *CFTR* is a chloride ion channel gene that plays a crucial role in homeostasis of various epithelia, especially in the intestine where it maintains chloride and bicarbonate secretion and fluid homeostasis (De Lisle & Borowitz, 2013). The *CFTR* gene is highly expressed in the mucosa of the intestine, with a decreasing gradient of expression along the base of the crypt to the tip axis. Mutations in the *CFTR* gene lead to cystic fibrosis, the most common autosomal recessive disorder in Caucasians (Cystic Fibrosis Foundation Patient Registry, as cited in Crites *et al*., 2015). Cystic fibrosis (CF) leads

to impaired chloride ion channel function and dysregulation of the epithelial fluid transport (De Lisle & Borowitz, 2013). Particularly in the mucosa of the intestine, impaired chloride ion channel function causes incomplete clearance and thick mucus, creating an environment for abnormal microbial colonization which can lead to microbial dysbiosis.

The Relationship between Cystic Fibrosis and Colorectal Cancer

A 20-year nationwide study has found an increased risk of digestive tract cancers, including small intestinal and colorectal cancer, in CF patients (Maisonneuve, Marshall, Knapp & Lowenfels, 2012). A study conducted by the Minnesota Cystic Fibrosis Center analyzed the results of colonoscopies after age 40 (Niccum, Billings, Dunitz & Khoruts, 2016). More than 50% of CF patients had adenomatous polyps, and about 25% of them had advanced adenomas. Early and high incidences of adenomas were found in CF patients.

Identification of *CFTR* as a Tumor Suppressor in Human and Murine Colorectal Cancer

To confirm the role of *CFTR* in colon cancer, our lab has studied *CFTR* deficiency in various mouse models and in human CRC patients. In 2016, our lab published that *CFTR* is a tumor suppressor in murine and human CRC (Than *et al*., 2016). A previous member of our lab, Bich L. N. Than, explored the influence of *CFTR* dysregulation on intestinal cancer by using Apc^{Min} mice with an intestinal-specific knockout (KO) of *Cftr*. An Apc^{Min} mouse has a point mutation in the homolog of the *APC* tumor suppressor gene (Moser *et al.*, 1993). Than et al. (2016) found more tumors developed

in the small intestines and colons in *Cftr* mutant Apc^{Min} mice than in *Cftr* wild-type Apc^{Min} mice. In addition, they found that the loss of *Cftr* induced intestinal tumors in >60% of one year old $Apc^{+/+}$ mice.

Than et al. (2016) performed RNA Seq analysis of tumors from *Cftr* mutant $Apc^{+/+}$ mice. RNA Seq is used for transcriptome profiling. It converts mRNA to cDNA fragments, performs short-read sequencing to these cDNA fragments, aligns these sequences with the reference genome or transcriptome, and allows quantification of the relative expression of genes in the sample (Parker *et al.*, 2017; Wang, Gerstein & Snyder, 2009). The mRNA from tumors from *Cftr* mutant $Apc^{+/+}$ mice was compared with mRNA from tumors from *Cftr* mutant Apc^{Min} mice and *Cftr* wild-type Apc^{Min} mice, and with mRNA from normal tissues from *Cftr* mutant $Apc^{+/+}$ mice and *Cftr* wild-type $Apc^{+/+}$ mice. RNA Seq identified dysgulation of several sets of genes including altered target genes of the Wnt β-catenin signaling and altered genes relating to the intestinal stem cell compartment (ISC) in tumors from *Cftr* mutant $Apc^{+/+}$ mice compared to normal tissues from *Cftr* mutant $Apc^{+/+}$ mice (Than *et al*., 2016). Gene set enrichment analysis (GSEA) was performed to evaluate the enrichment or depletion of gene sets in the *Cftr* depletion samples compared to the no depletion samples. GSEA is a computational method used to identify gene sets that are significantly altered in a given dataset (in a biological state) (Broad Institute, 2018). GSEA found an overlap in tumors from *Cftr* mutant $Apc^{+/+}$ mice for ISC genes enriched in tumors from *Cftr* wild-type Apc^{Min} mice (Than *et al*., 2016). Microarray experiments were conducted to simultaneously compare the different gene expression levels of a large set of genes

between the *Cftr* depletion samples and the no depletion samples. Microarray experiments require the conversion of mRNA to cDNA fragments which undergo attachment to fluorescent markers and reaction with DNA probes, allowing for identification of target DNA via fluorescence (Govindarajan, Duraiyan, Kaliyappan & Palanisamy, 2012). Microarray analysis identified dysregulation of genes involved in the ion channel, immune responses, and cell fate decisions in normal tissues from *Cftr* mutant $Apc^{+/+}$ mice (Than *et al*., 2016). Ingenuity Pathway Analysis (IPA) on microarray data was performed to identify pathways relating to or reacting with dysregulated gene expression (Jiménez-Marín, Collado-Romero, Ramirez-Boo, Arce & Garrido, 2009) following *Cftr* depletion. Applying this web-based software allowed for the identification of pathways that are altered in normal tissues from *Cftr* mutant $Apc^{+/+}$ mice and further changed in tumors from *Cftr* mutant $Apc^{+/+}$ mice. The analysis found an overlap for genes involved in lipid metabolism and immune responses (Than *et al*., 2016).

After that, Than et al. (2016) studied the correlation between *CFTR* expression and disease-free survival in CRC patients. The early stage human CRC patients were stratified by tumor *CFTR* gene expression, and risk of relapse in each group was determined. The data showed that in the microsatellite stable (MSS) subset, the three-year relapse free survival in the *CFTR* high-expressing human CRC patients was 85%, while the three-year relapse free survival in the *CFTR* low-expressing human CRC patients was 56%, suggesting that *CFTR* deficiency was significantly correlated with lower disease-free survival (Than *et al*., 2016). The MSS is a subset of CRC, and MSS

tumors occur in 80-85% of CRC patients and do not respond to immunotherapies due to an already deficient immune response (Zhao, May, Lou & Subramanian, 2018).

The Focus of this Project

CFTR is a tumor suppressor for CRC (Than *et al*., 2016), but the mechanism by which *CFTR* prevents colorectal cancer is unknown. Our lab is trying to determine that mechanism and provide knowledge that can lead to new therapies for colorectal cancer. This project is focused on the unfolded protein response (UPR). This is because GSEA pathway analysis showed that *CFTR*-deficient normal and tumor tissues from mice and humans were enriched in genes involved in the UPR signaling pathway.

Background on Unfolded Protein Response

The main tasks of the endoplasmic reticulum (ER) include maintaining intracellular Ca^{2+} homeostasis and protein folding and transport (Corazzari, Gagliardi, Fimia & Piacentini, 2017). Altered ER homeostasis leads to the accumulation of unfolded or misfolded proteins, a condition called ER stress (Kaufman & Wang, 2016). The UPR is initiated in response to ER stress. Through activating a series of signaling pathways, UPR can increase the production of chaperones, reduce the synthesis of unfolded proteins, and increase the degradation of unfolded proteins (Kaufman & Wang, 2016). However, if the ER stress exceeds the functional capacity of the ER, the cell will enter apoptosis, or programmed cell death (Kaufman & Wang, 2016).

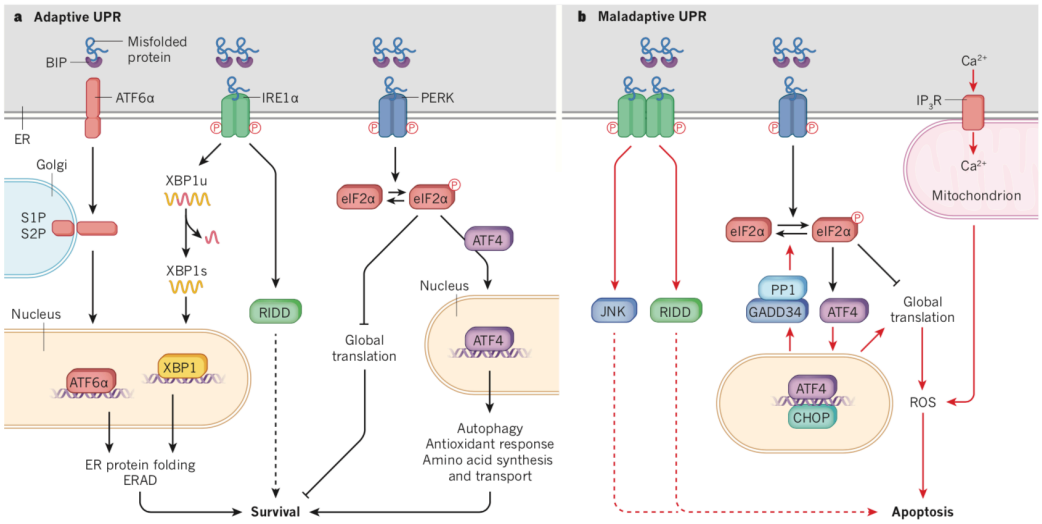

Figure 3. Adaptive and maladaptive UPR signaling pathways (Kaufman & Wang, 2016).

UPR activation can be adaptive and maladaptive in eukaryotic cells (Figure 3; Kaufman & Wang, 2016). When unfolded proteins bind to heat shock protein A member 5 (HSPA5), which is also called GRP78 or BIP, three molecules are released. These molecules are activating transcription factor 6 alpha (ATF6α), inositol-requiring protein 1 alpha (IRE1α), and protein kinase PKR-like ER kinase (PERK), and activate certain signaling pathways (Ni & Lee, 2007). The activation of IRE1α can lead to the alternative splicing of transcription factor X-box binding protein 1 (*XBP1*) transcripts (Lerner *et al.,* 2012; Yoshida *et al.,* 2001). The cleavage of ATF6α produces a transcriptionally active fragment (Lee *et al.*, 2002). As a result, transcriptional response regulates the expression of genes involved in ER protein folding, increasing the capacity of the ER (Kaufman & Wang, 2016). Sensing ER stress activates the kinase function of PERK, phosphorylating the elongation initiation factor 2α (eIF2α)

(Kaufman & Wang, 2014). The phosphorylation of eIF2α promotes a pro-adaptive signal by suppressing global protein synthesis and selectively increasing activating transcription factor 4 (*ATF4*) transcripts that direct synthesis and transport of amino acids and temporary translation attenuation (Kaufman & Wang, 2014). As adaptive UPR, these three signaling pathways increase the capacity of the ER and contribute to cell survival.

In contrast, maladaptive UPR ensues when hyperactivated irremediable ER stress exceeds the adaptive UPR capacity (Kaufman & Wang, 2016). Prolonged and severe ER stress can activate the PERK signaling pathway over time. EIF2α phosphorylation halts global translation including the synthesis of anti-apoptotic Bcl-2 proteins; ATF4 directs transcription of the CCAAT/enhancer binding homologous protein (*CHOP*) gene, promoting programmed cell death (Hetz, 2012). IRE1α hyperactivation increases the thioredoxin-interacting protein (*TXNIP*) level by destabilizing its negative regulator, miR-17 (Lerner *et al.,* 2012). The *TXNIP* gene encodes pro-oxidant protein which induces inflammation and cell death, and has been reported to contribute to the switch from adaptive to maladaptive UPR (Oslowski *et al.,* 2012; Lerner *et al.,* 2014). IRE1α activation recruits TNF-receptor-associated factor 2 (TRAF2) and Iκ kinase, contributing to the phosphorylation of c-Jun N-terminal kinase (JNK) (Urano *et al.*, 2000) and NF-κB (Hu, Han, Couvillon, Kaufman & Exton, 2006), respectively. As a result, the maladaptive UPR can be activated, which can lead to apoptosis. In addition, the ER stress-mediated leakage of calcium into the cytoplasm might result in the activation of death effectors, activating the apoptotic pathway (Rozpedek *et al.*, 2016).

UPR in the Human Intestinal Secretory Cells

At the mucosal interface with the microbial milieu, intestinal epithelial cells are stimulated to secrete a large amount of proteins (Kaser, Flak, Tomczak & Blumberg, 2011). The excessive accumulation of unfolded proteins in the ER induces ER stress in the secretory cells (Kaser, Flak, Tomczak & Blumberg, 2011). The most important secretory cells in the intestine are Paneth cells and goblet cells (Kaser, Flak, Tomczak & Blumberg, 2011). Paneth cells have two delivery functions: they deliver signals on which the proliferation of stem cells relies, and they transport antimicrobial peptides into the lumen (Kaser, Flak, Tomczak & Blumberg, 2011). The goblet cells are responsible for the production and secretion of gel-forming mucins, which are used to protect mucosal membranes (Kaser, Flak, Tomczak & Blumberg, 2011). Highly secretory cells are vulnerable to ER stress, and these cells depend on a proper UPR for their secretory activities and homeostasis (Kaser & Blumberg, 2009). Genetic alterations including the impaired expression of genes involved in the adaptive ER function can damage the function of the UPR or cause the accumulation of unfolded proteins in the ER (Kaser *et al.*, 2008). The unsolved and accumulated ER stress might exceed the functional capacity of the adaptive UPR. This disruption can lead to apoptosis, loss of Paneth and goblet cells, loss of mucosal barrier function, and inflammation (Kaser *et al.*, 2008).

UPR in the Intestinal Stem Cells

Because cancer stem cells develop from oncogenic mutations in intestinal stem cells, CRC research is focused on the impact of the ER stress-induced UPR on the cell

fate of intestinal stem cells. Stem cells cycle and generate transit-amplifying cells capable of cycling and differentiating toward all lineages in the intestinal epithelium (Clevers, 2013). The unfolded protein response is activated and required when intestinal stem cells normally differentiate (Heijmans *et al*., 2013). Cell differentiation demands a variety of specialized proteins, which needs ER to process the accumulated unfolded proteins (Heijmans *et al*., 2013). ER stress-induced UPR makes intestinal stem cells lose their self-renewal capacity and differentiate (Heijmans *et al*., 2013). To maintain stemness capacity, intestinal stem cells need to reduce high levels of UPR activation. Otherwise, intestinal stem cells will be removed by differentiation.

UPR in Cancer Cells

Increased unfolded protein synthesis in cancer cells often creates increased ER stress and UPR activation (Dejeans, Barroso, Fernandez-Zapico, Samali, Chevet, 2015). Mutations in oncogenes or tumor suppressors lead to the accumulation of unfolded proteins, activating UPR (Kaufman & Wang, 2014). Cancer cells proliferate and metastasize quickly and thus face a hostile environment with limited oxygen and nutrients, which disrupts ER homeostasis, induces ER stress and activates UPR (Kaufman & Wang, 2014; Ma & Hendershot, 2004). Tumors that survive the environmental stress possess high UPR activation (Chevet, Hetz & Samali, 2015).

High UPR activity is believed to give cancer cells a survival advantage (Chevet, Hetz & Samali, 2015). According to the hallmarks of cancer, cancer cells can activate pathways to support the growth and survival of tumor cells (Hanahan & Weinberg, 2011). Higher levels of UPR lead to the death of normal cells, but some cancer cells

protect themselves from and adapt to ER stress (Chevet, Hetz & Samali, 2015). The activated UPR can increase protein folding and the secretion of cytokines, angiogenesis factors, and extracellular matrix components, supporting the growth and survival of cancer cells (Corazzari, Gagliardi, Fimia & Piacentini, 2017).

The Goal of This Project

We hypothesize that the loss of *CFTR* increases protection from ER stress and that this protection supports the survival of CRC cells. To conceptualize a mechanism by which *CFTR* deficiency leads to CRC, a working model is proposed that UPR activation is enhanced in *CFTR* KO cells, and this activation contributes to CRC cell survival under ER stress. To test the hypothesis and evaluate the working model, a pair of *CFTR* knockout (KO) and wildtype (WT) Caco2 cell lines were used to test the correlation between UPR and cancer-supporting effects of *CFTR*-deficiency. These cell lines were created by CRISPR-Cas9 engineering by our collaborator Dr. Mitchell Drumm at Case Western Reserve University. Caco2 is a colon adenocarcinoma cell line commonly used as a model of the intestinal absorptive and defensive mucosa monolayer, and it has abundant *CFTR* expression (Sood *et al.*, 1992; Borchardt, 2011). The goal of this project is to evaluate the working model by analyzing gene expression and utilizing cell viability assays.

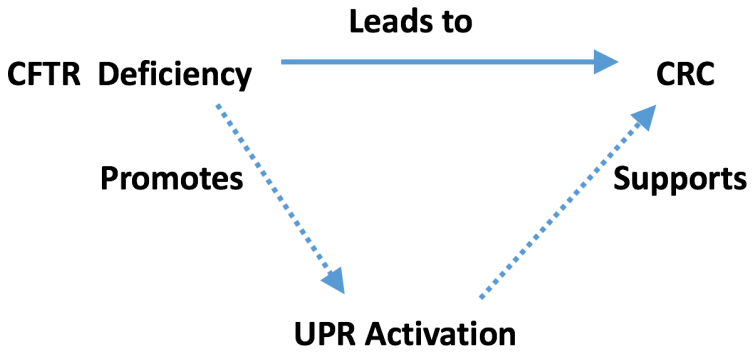

Figure 4. Working model.

Results

We hypothesized that loss of *CFTR* increases UPR activation, and that this activation supports the survival of CRC cells under ER stress. To investigate the mechanism underlying CRC suppression by *CFTR*, a pair of *CFTR* knockout (KO) and wildtype (WT) Caco2 cell lines were utilized to test the correlation between UPR and the cancer-supporting effects of *CFTR*-deficiency. We hypothesized that the loss of *CFTR* might increase UPR activation. To evaluate the UPR activities in *CFTR* KO cells, RT-qPCR analysis was performed to examine the gene expression changes involved in the UPR signaling pathway.

RT-qPCR for *CFTR* Validates *CFTR* KO Cells

Initially, it was necessary to confirm that *CFTR* expression is relatively low in *CFTR* KO cells. *CFTR* KO and WT Caco2 cell lines were created by CRISPR-Cas9 engineering by our collaborator Dr. Mitchell Drumm at Case Western Reserve University. A frameshift mutation occurs in the exon 11 in the coding region of *CFTR* on chromosome 7 in *CFTR* KO cells. RT-qPCR was conducted to evaluate the expression of *CFTR* in the *CFTR* KO and WT Caco2 cell lines. One million (10^6) *CFTR* WT and *CFTR* KO Caco2 cells were plated into 60 mm tissue culture dishes and cultured overnight, and total RNA was extracted from the *CFTR* WT and *CFTR* KO Caco2 cells. The *CFTR* mRNA expression levels were determined by RT-qPCR. To minimize technical variations, the expression of *CFTR* was normalized to the expression of 18S. The results showed that the expression of *CFTR* in *CFTR* KO cells

was lower than in *CFTR* WT cells (Figure 5). RT-qPCR for *CFTR* verifies *CFTR* KO cells.

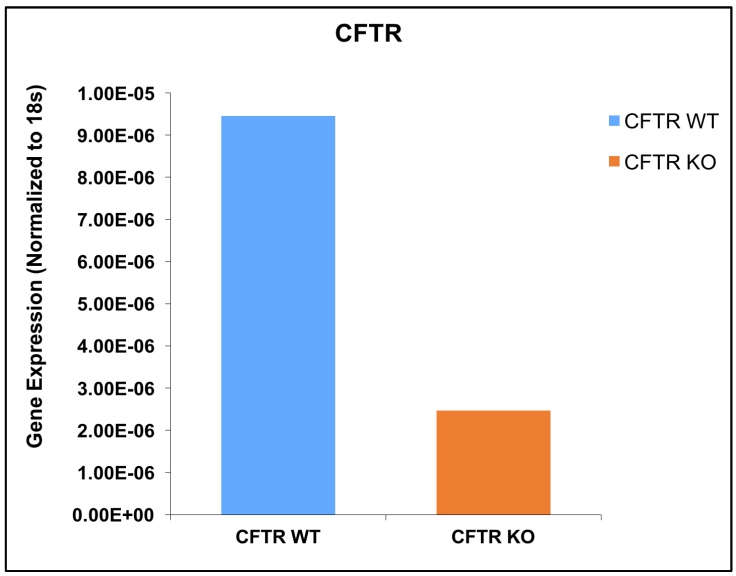

Figure 5. Expression of *CFTR in CFTR* WT and *CFTR* KO Caco2 cell lines. *CFTR* mRNA expression in *CFTR* WT and *CFTR* KO cells was measured by RT-qPCR. The expression of *CFTR* was normalized to the expression of 18S.

The Expression of Genes Associated with UPR in *CFTR* WT and *CFTR* KO Caco2 Cell Lines

We hypothesized that the loss of *CFTR* might increase the UPR activation. To assess the UPR activities in *CFTR* KO and WT cells, RT-qPCR analysis was conducted to compare the gene expression changes involved in the UPR signaling pathway in *CFTR* WT and *CFTR* KO Caco2 cell lines. To compare the mRNA expression of genes relating to the UPR signaling pathway in *CFTR* WT and *CFTR* KO cells, one million (10^6) *CFTR* WT and *CFTR* KO Caco2 cells were plated into 60 mm tissue culture dishes and cultured overnight, and total RNA was extracted from *CFTR* WT and *CFTR* KO Caco2 cells. The mRNA expression levels were determined by RT-qPCR. To

evaluate the UPR activities in *CFTR* KO cells under ER stress, RT-qPCR analysis was performed to compare the gene expression changes involved in the UPR signaling pathway in *CFTR* WT and *CFTR* KO Caco2 cell lines treated with Thapsigargin (TG) to induce ER stress. To compare the mRNA expression of genes relating to the UPR signaling pathway in *CFTR* WT and *CFTR* KO cells treated with inducers to trigger ER stress, one million (10^6) *CFTR* WT and *CFTR* KO Caco2 cells were plated into 60 mm tissue culture dishes, cultured overnight, treated with 0.2 μM TG for 2.5 hours, and total RNA was extracted from DMSO controls and treated *CFTR* WT and *CFTR* KO Caco2 cells. TG inhibits sarcoplasmic/endoplasmic reticulum Ca^{2+}-ATPase (SERCA) and breaks down ER Ca^{2+} gradient (Oslowski & Urano, 2011). The lower calcium levels in the ER disrupt dependent chaperone activities and induce ER stress (Oslowski & Urano, 2011). TG can be dissolved in DMSO, and the low concentration of DMSO was added to cells to serve as a no treatment control. The mRNA expression levels were determined by RT-qPCR. To minimize technical variations, the expression of each gene of interest was normalized to the expression of 18S. Each bar represents the mean, and error bars represent the standard deviation of 3 biological replicates, unless otherwise stated. A paired two-tailed *t*-test was used to determine the statistical significance of the entirety of the RT-qPCR data and MTT data in this thesis. All statistical tests used a significance value of $\alpha = 0.05$. Comparisons of $p \leq 0.05$ are marked by an asterisk *.

The *HSPA5* gene encodes the chaperone protein GRP78 that serves as the gatekeeper of UPR (Zhu & Lee, 2015). Sensing of ER stress dissociates GRP78 from

ATF6α, IRE1α and PERK, initiating all three UPR sub-pathways (Kaufman & Wang, 2016). The *HSPA5* expression levels in *CFTR* WT and *CFTR* KO cells were analyzed. The basal levels of the *HSPA5* in *CFTR* WT and *CFTR* KO cells were not different (Figure 6a). The expression of the *HSPA5* was analyzed in *CFTR* WT and *CFTR* KO cells treated with TG as well as in untreated controls (Figure 6). To determine the effect of ER stress on gene expression in each cell line, the ratio of TG treated over untreated gene expression levels was analyzed (Figure 6b). The expression levels of the *HSPA5* gene in both *CFTR* WT and *CFTR* KO cells increased after TG treatment. The *HSPA5* expression levels were increased to 2.2 and 3.8-fold (Figure 6b), respectively, in *CFTR* WT and *CFTR* KO cells. The effect of the TG treatment on *HSPA5* expression in *CFTR* KO cells was more than the effect of the TG treatment on *HSPA5* expression in *CFTR* WT cells. The difference between the expression levels in WT and KO cells after treatment is not statistically significant at $p \leq 0.05$. A trend was suggested by these data that *CFTR* deficiency may raise the effect of TG-induced ER stress on the expression of the UPR gatekeeper *HSPA5*.

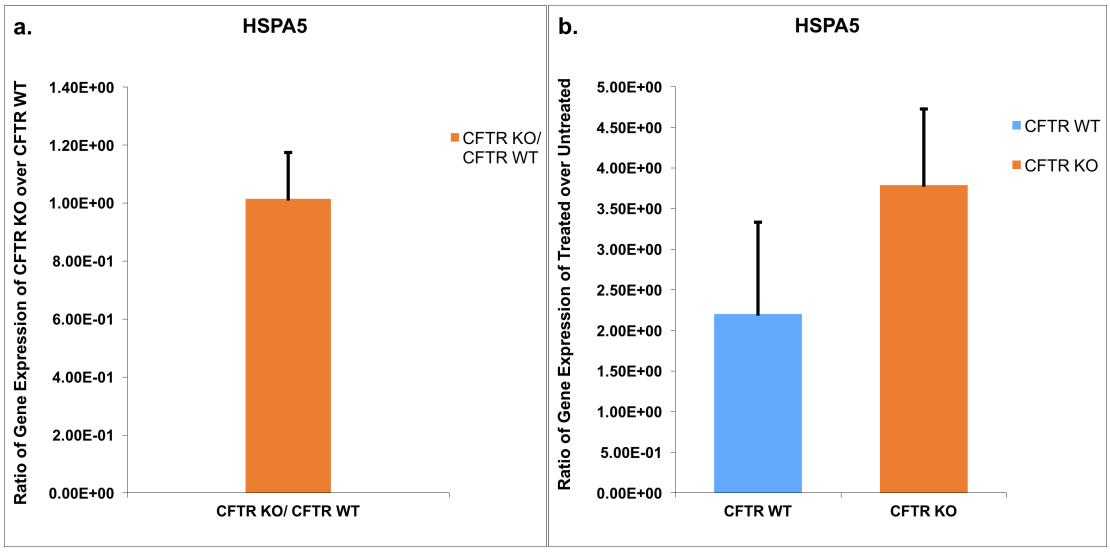

Figure 6. Expression of *HSPA5 in CFTR* WT and *CFTR* KO Caco2 cell lines. *HSPA5* mRNA expression (a) (b) was measured by RT-qPCR. The expression of *HSPA5* was normalized to the expression of 18S. (a) The Y-axis refers to the ratio of *CFTR* KO cells over *CFTR* WT cells gene basal expression levels. (b) The Y-axis refers to the ratio of TG treated over untreated gene expression levels.

The PERK signaling target *ATF4* transcripts regulate the synthesis and transport of amino acids and temporary translation attenuation (Kaufman & Wang, 2014). *ATF4* expression levels in *CFTR* WT and *CFTR* KO cells were analyzed. The basal levels of *ATF4* in *CFTR* WT and *CFTR* KO cells were not different (Figure 7a). The expression of *ATF4* was analyzed in *CFTR* WT and *CFTR* KO cells treated with TG as well as in untreated controls. To determine the effect of ER stress on gene expression in each cell line, the ratio of TG treated over untreated gene expression levels was analyzed (Figure 7b). The expression levels of the *ATF4* gene in both *CFTR* WT and *CFTR* KO cells increased after TG treatment. *ATF4* expression levels increased to the same extent in both *CFTR* WT and *CFTR* KO cells (Figure 7b). These data indicate that the loss of

CFTR might not influence the effect of TG-induced ER stress on the expression of PERK signaling target gene *ATF4*.

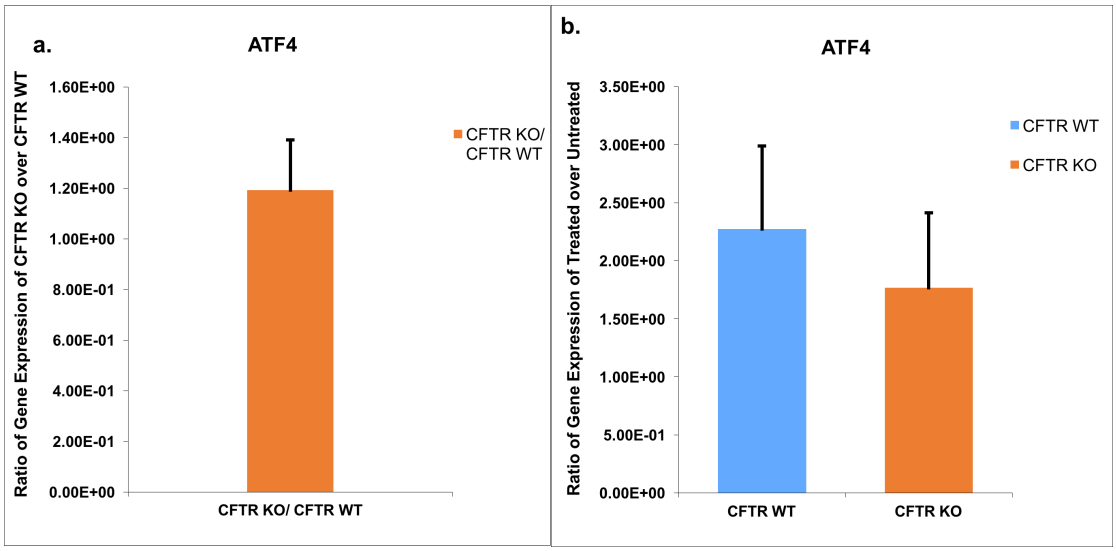

Figure 7. Expression of *ATF4 in CFTR* WT and *CFTR* KO Caco2 cell lines. *ATF4* mRNA expression (a) (b) was measured by RT-qPCR. The expression of *ATF4* was normalized to the expression of 18S. (a) The Y-axis refers to the ratio of *CFTR* KO cells over *CFTR* WT cells gene basal expression levels. (b) The Y-axis refers to the ratio of TG treated over untreated gene expression levels.

Wang and Kaufman (2016) state that the three UPR sub-pathways are not simultaneously activated by ER stress, thus it is of interest to evaluate the activities of other UPR signaling branches. To evaluate IRE1α activities in CFTR KO cells, RT-qPCR analysis was performed to assess gene expression changes involved in the IRE1α signaling pathway. To compare the mRNA expression of genes relating to the IRE1α signaling pathway in *CFTR* WT and *CFTR* KO cells, one million (10^6) Caco2 cells were plated into 60 mm tissue culture dishes, cultured overnight, and total RNA was extracted from *CFTR* WT and *CFTR* KO Caco2 cell lines without artificially sustained ER stress. The mRNA expression levels were determined by RT-qPCR.

The expression of total *XBP1* was analyzed in *CFTR* WT and *CFTR* KO Caco2 cell lines (Figure 8) by Amanda Palme. Under remediable ER stress, IRE1α activation restricts its carboxy-terminal ribonuclease activity toward the mRNA encoding XBP-1, leading to the alternative splicing of *XBP1* unspliced mRNA (Lerner *et al.,* 2012; Yoshida *et al.,* 2001). The *XBP1* spliced mRNA is translated to an active transcription factor that triggers the expression of genes involved in adaptive functions such as protein folding, protein quality control, phospholipid synthesis, and ER-associated degradation of misfolded proteins (Hetz, Martinon, Rodriguez & Glimcher, 2011). In this experiment, the expression of *XBP1* in *CFTR* WT cells was higher than the expression of *XBP1* in *CFTR* KO cells (Figure 8). The ratio of *XBP1* levels in *CFTR* KO cells over *CFTR* WT cells is 0.58. The difference between the expression levels in WT and KO cells is not statistically significant at $p \leq 0.05$. A trend was suggested by these data that the loss of *CFTR* might decrease total *XBP1* expression.

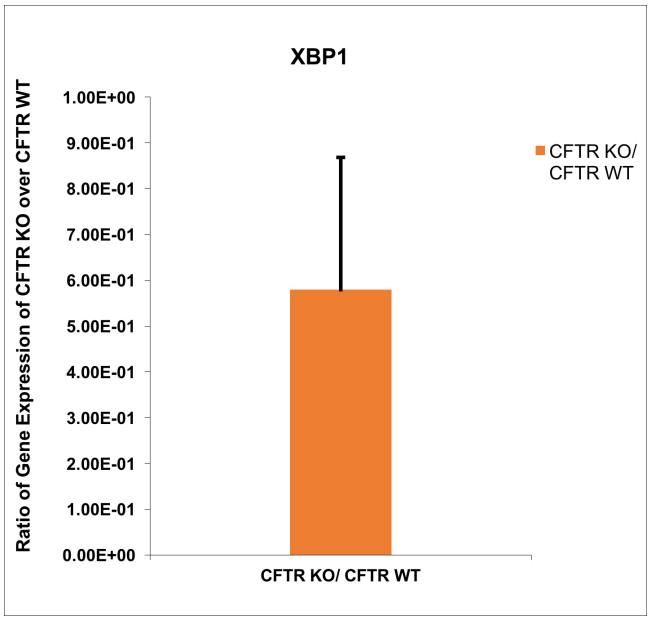

Figure 8. Expression of *XBP1 in CFTR* WT and *CFTR* KO Caco2 cell lines. *XBP1* mRNA expression was measured by RT-qPCR. The expression of *XBP1* was normalized to the expression of 18S. The Y-axis refers to the ratio of *CFTR* KO cells over *CFTR* WT cells gene expression levels.

The expression of thioredoxin-interacting protein (*TXNIP*) was analyzed in *CFTR* WT and *CFTR* KO Caco2 cell lines (Figure 9) by Amanda Palme. Under excessive ER stress, IRE1α activation enhances *TXNIP* levels by destabilizing miR-17 (Lerner *et al.,* 2012). The *TXNIP* gene encodes pro-oxidant proteins leading to inflammation and cell death and has been reported to contribute to the switch from adaptive to maladaptive UPR (Oslowski *et al.,* 2012; Lerner *et al.,* 2014). In this experiment, *CFTR* WT cells had an increased expression of *TXNIP* than *CFTR* KO cells (Figure 9). The ratio of TNXIP levels in *CFTR* KO cells over *CFTR* WT cells is 0.32. The standard deviation of 2 biological replicates is 0.018. The difference between the expression levels in WT and KO cells is statistically significant at $p \leq 0.05$ ($p=0.012$). These data suggest that

the loss of *CFTR* results in a decrease in the expression of *TXNIP*.

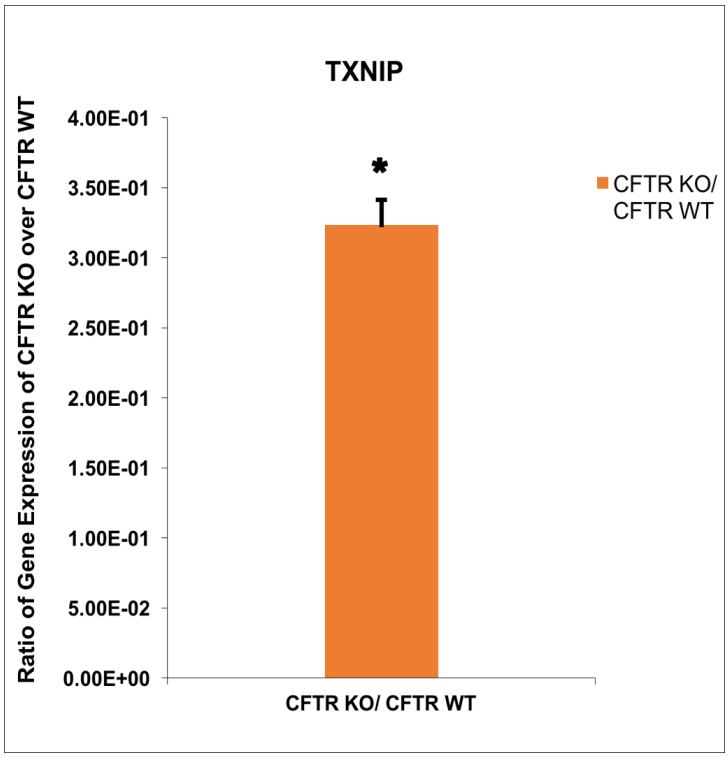

Figure 9. Expression of *TXNIP in CFTR* WT and *CFTR* KO Caco2 cell lines. *TXNIP* mRNA expression was measured by RT-qPCR. The expression of *TXNIP* was normalized to the expression of 18S. The Y-axis refers to the ratio of *CFTR* KO cells over *CFTR* WT cells gene expression levels. The standard deviation for two biological replicates is shown by the error bars. Statistical significance was determined by a paired two-tailed *t*-test. * = $p < 0.05$.

To determine if the loss of *CFTR* enhances UPR activation, we examined the effect of *CFTR* deficiency on expression of genes involved in the UPR activities. The increased effect of TG treatment on *HSPA5* expression in *CFTR* KO suggests a trend that the loss of *CFTR* might enhance the effect of ER stress on the expression of the UPR gatekeeper *HSPA5,* the common regulator for initiating three UPR sub-pathways. The increase to the same extent in *ATF4* expression in both *CFTR* WT and *CFTR* KO cells reflects that the loss of *CFTR* might not enhance the activation of PERK

signaling. The decreased levels of total *XBP1* mRNA in *CFTR* KO cells reflect that *CFTR* deficiency might not activate the IRE1α signaling pathway. *TXNIP*, which is part of an apoptotic pathway, is down-regulated in *CFTR* KO cells. This down regulation might provide protection from apoptosis. Together, these studies suggest that UPR activation might be up-regulated in *CFTR* KO cells, but the specific pathway might not be the one addressed in this study. In addition, the down regulation of *TXNIP* might offer protection for cancer cells from apoptosis. Except the *TXNIP*, these data from these three genes did not show a statistically significant difference. More studies are required to evaluate UPR activities in *CFTR* WT and *CFTR* KO cells and thereby support or refute our hypotheses.

Cell Viability of *CFTR* WT and *CFTR* KO Caco2 Cell Lines

Although many cancer cells require an enhanced UPR, excessive prolonged activation triggers a switch to an apoptotic pathway (Wang & Kaufman, 2016; Niederreiter, L. *et al.,* 2013). To detect if the loss of *CFTR* protects the survival of CRC cells in the presence of hyperactivated irremediable ER stress, cell viability of *CFTR* KO and WT cells under ER stress was compared. The initial step was to compare the cell viability of *CFTR* WT and *CFTR* KO Caco2 cell lines before TG treatment by using the MTT assay. Twenty-five hundred (2,500) Caco2 cells per well, 5,000 Caco2 cells per well and 10,000 Caco2 cells per well with 6 technical replicates were plated into 96 well plates and cultured from 18 hours to 90 hours in 1 biological replicate. Cell viability was determined by the MTT assay. The cell viability of the *CFTR* WT Caco2 cells before TG treatment was higher than that of the *CFTR* KO Caco2 cells over the

duration of plating (Figure 10). These data reflect the variations between cell growth of the two cell lines.

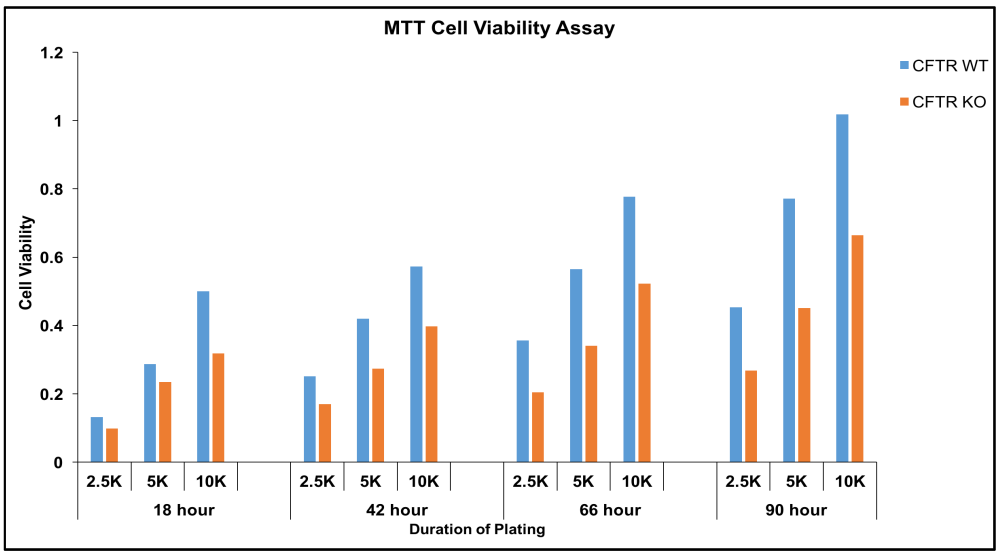

Figure 10. MTT cell viability assay in *CFTR* WT and *CFTR* KO Caco2 cell lines. The cell viability of *CFTR* WT and *CFTR* KO Caco2 cell lines was measured by the MTT assay. The Y axis refers to absorbance which reflects cell viability.

To evaluate if the loss of *CFTR* protects the survival of CRC cells in the presence of excessive ER stress, the MTT assay was performed to compare cell viability of *CFTR* KO and WT cells treated with TG to induce ER stress. A dose gradient was utilized to select the concentration of TG used for treatment. Ten thousand (10,000) Caco2 cells per well with 6 technical replicates were plated into 96-well plates, cultured overnight and treated with TG. Cells were treated with different doses of TG (0.2µM, 0.4µM, 0.8µM) from 2 hours to 72 hours in 1 biological replicate. Cell viability was determined by the MTT assay. The ratio of treated over untreated viability of both *CFTR* KO and WT cells decreased over the duration of TG treatment from 2 hours to 72 hours (Figure 11). We chose 0.2 µM TG to treat Caco2 cells because it is

the lowest dose that affects the cell viability of *CFTR* KO and WT Caco2 cell lines within 72 hours in this experiment (Figure 11).

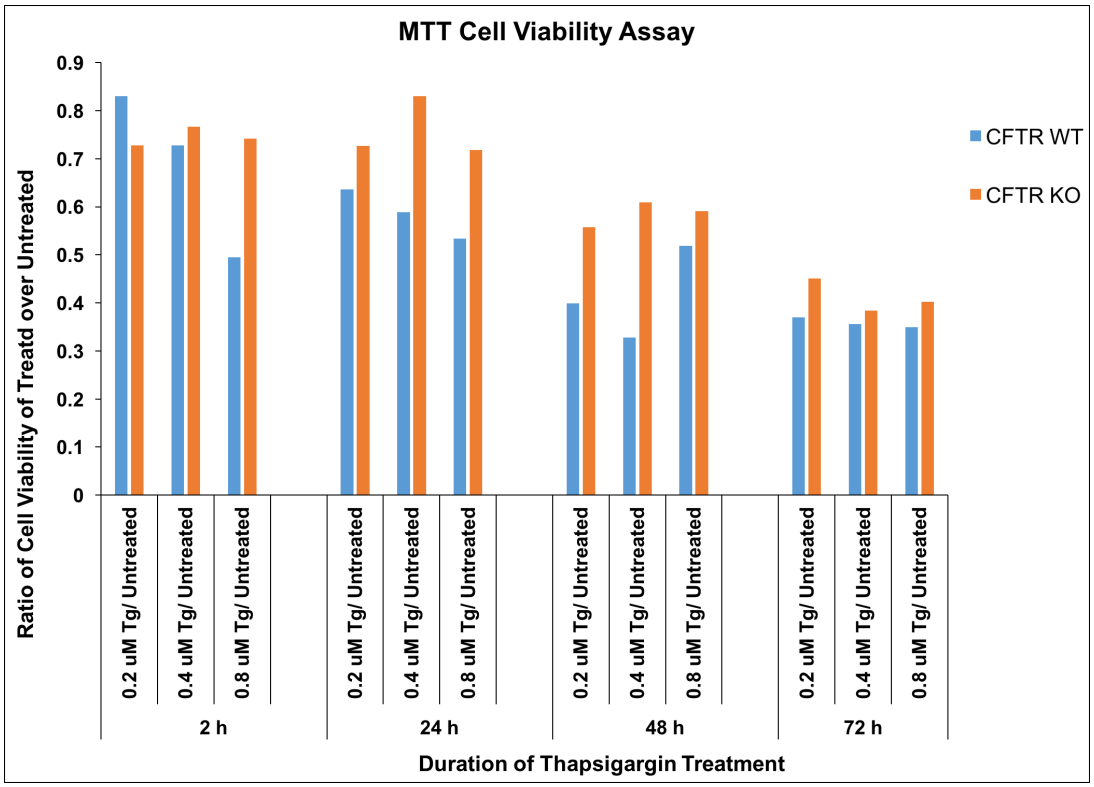

Figure 11. MTT cell viability assay in *CFTR* WT and *CFTR* KO Caco2 cell lines after TG treatment. The cell viability of *CFTR* WT and *CFTR* KO Caco2 cell lines after treatment with different doses of TG, as indicated, was measured by the MTT assay from 2 hours to 72 hours. The Y-axis refers to the ratio of treated over untreated viability of Caco2 cell lines.

To evaluate if the *CFTR* deficiency promotes the survival of CRC under hyperactivated irremediable ER stress, the MTT assay was conducted to compare the cell viability of *CFTR* KO and WT Caco2 cell lines treated with TG to induce ER stress. Five thousand (5,000) Caco2 cells per well with 6 technical replicates were plated into 96 well plates, cultured overnight and treated with TG. Cells were treated with 0.2μM TG from 3 hours to 72 hours. Cell viability was determined by the MTT

assay. The previous experiment suggested that the cell viability of *CFTR* WT and *CFTR* KO cells differ between plating. For the analysis in this experiment, MTT values at each point were normalized to 3 hour untreated controls for *CFTR* WT and *CFTR* KO cells to control the variations in plating. To determine the effect of ER stress on each cell line, the ratio of treated over untreated viability at each point was analyzed. The TG treatment gave rise to decreased cell viability in both *CFTR* WT and *CFTR* KO cells over time. The cell viability decreased to about 26% and 43%, respectively, in *CFTR* WT and *CFTR* KO cells at 72 hours. The ratio of treated over untreated viability was higher in *CFTR* KO cells than that in WT cells (Figure 12). The difference between the ratios in WT and KO cells is statistically significant at $p \leq 0.05$ ($p=0.049$, Figure 12). These data indicate that *CFTR* deficiency causes TG-induced ER stress to have less of an effect on cell viability.

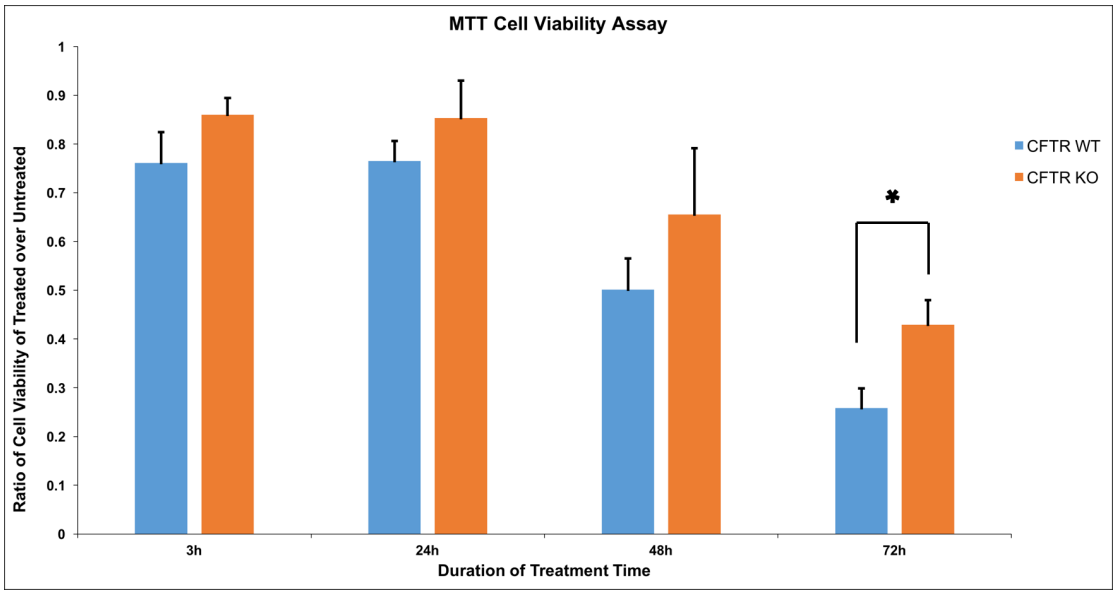

Figure 12. MTT cell viability assay in *CFTR* WT and *CFTR* KO Caco2 cell lines after TG treatment. The cell viability of *CFTR* WT and *CFTR* KO Caco2 cell lines after treatment with TG was measured by the MTT assay from 3 hours to 72 hours. The Y-axis refers to the ratio of treated over untreated viability of Caco2 cell lines. Statistical significance of differences in cell viability at each time point was determined by a paired two-tailed *t*-test. The difference at 72 hours was found to be statistically significant.
* = $p \leq 0.05$.

To evaluate if *CFTR* deficiency supports the survival of CRC cells under excessive ER stress, the MTT assay was conducted to compare the cell viability of *CFTR* KO and WT Caco2 cell lines treated with another inducer, Tunicamycin (TM), to trigger ER stress. TM suppresses UDP-N-acetylglucosamine-dolichol phosphate N-acetylglucosamine-1-phosphate transferase (GPT) and thus halts the initiation of glycoprotein biosynthesis in the ER (Oslowski & Urano, 2011). The unglycosylated proteins cannot leave the ER, so there is an accumulation causing ER stress (Oslowski & Urano, 2011). Twenty thousand (20,000) Caco2 cells per well with 6 technical

replicates were plated into 96-well plates, cultured overnight and treated with TM. Cells were treated with different doses of TM (2.5 μg/ml, 5 μg/ml, 10 μg/ml) from 2 hours to 72 hours in 1 biological replicate. Cell viability was determined by the MTT assay. For analysis, MTT values at each point were normalized to 0 hour untreated controls for *CFTR* WT cells and *CFTR* KO cells to control the variations in plating. To determine the effect of ER stress on each cell line, the ratio of treated over untreated viability at each point was analyzed. The TM treatment resulted in dose- and time-dependent decreases in cell viability in both *CFTR* WT and *CFTR* KO cells (Figure 13). The ratio of treated over untreated viability was higher in *CFTR* KO cells at 72 hours than in WT cells (Figure 13). The difference between the ratios in WT and KO cells is not statistically significant at $p \leq 0.05$. A trend has been suggested by these data that *CFTR* deficiency causes TM-induced ER stress to have less of an effect on cell viability.

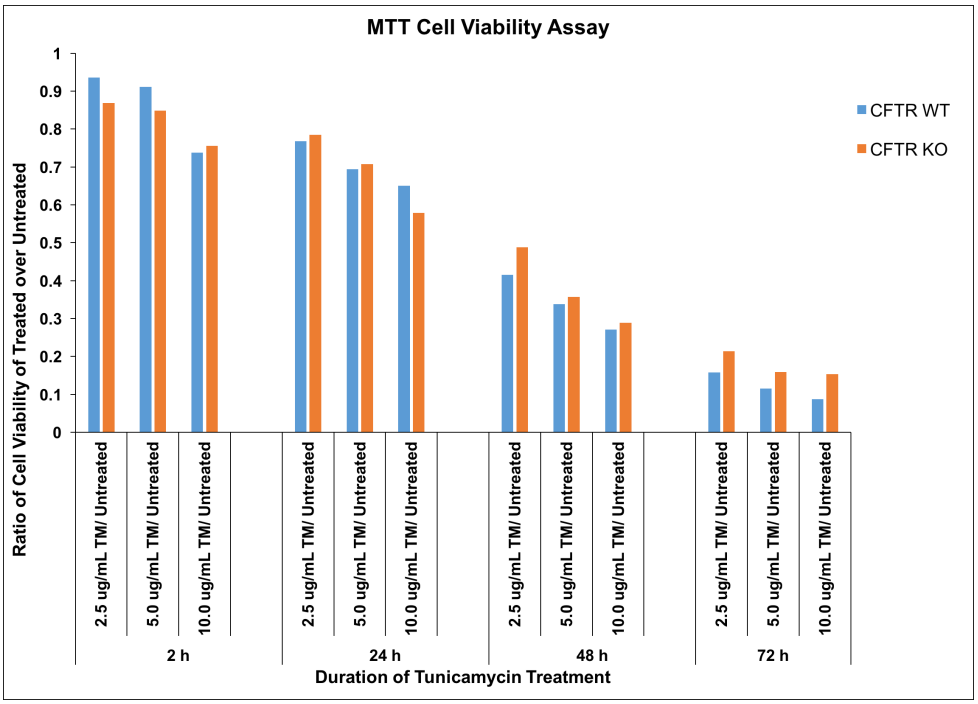

Figure 13. MTT cell viability assay in *CFTR* WT and *CFTR* KO Caco2 cell lines after TM treatment. The cell viability of *CFTR* WT and *CFTR* KO Caco2 cell lines after treatment with different doses of TM, as indicated, was measured by the MTT assay from 2 hours to 72 hours. The Y-axis refers to the ratio of treated over untreated viability of Caco2 cell lines.

To evaluate the relationship between *CFTR* deficiency and protection for CRC cells from ER stress, we compared the cell viability of *CFTR* KO and WT cells treated with two different inducers, TG and TM, to induce ER stress. The higher ratio of treated over untreated viability in *CFTR* KO cells suggests that the loss of *CFTR* causes ER stress to have less effect on cell viability. These data indicate that the loss of *CFTR* might protect the survival of CRC cells under excessive ER stress.

Gene Expression Analysis of the NF-κB Signaling Pathway in *CFTR* WT and *CFTR* KO Caco2 Cell Lines

Grootjans et al. (2016) demonstrated that ER stress-induced UPR activates the NF-κB signaling pathway. Recent research shows that *CFTR* deficiency activates the NF-κB signaling pathway (Crites *et al.*, 2015). We hypothesized that *CFTR* deficiency positively affects the NF-κB signaling pathway in the presence of UPR. To assess the innate NF-κB activities in *CFTR* KO and WT cells, RT-qPCR analysis was performed to compare the gene expression changes involved in the NF-κB signaling pathway in *CFTR* WT and *CFTR* KO Caco2 cell lines. To compare the mRNA expression of genes relating to the NF-κB signaling pathway in *CFTR* WT and *CFTR* KO, one million (10^6) *CFTR* WT and *CFTR* KO Caco2 cells were plated into 60 mm tissue culture dishes and cultured overnight, and total RNA was extracted from *CFTR* WT and *CFTR* KO Caco2 cells. The mRNA expression levels were determined by RT-qPCR. To evaluate the NF-κB activity in *CFTR* KO cells in response to UPR, RT-qPCR analysis was conducted to compare the gene expression changes involved in NF-κB signaling pathway in *CFTR* WT and *CFTR* KO Caco2 cell lines treated with TG to trigger ER stress. To evaluate the mRNA expression of genes relating to the NF-κB signal in *CFTR* KO cells, one million (10^6) *CFTR* WT and *CFTR* KO Caco2 cells were plated into 60 mm tissue culture dishes, cultured overnight, treated with 0.2 μM TG for 2.5 hours, and total RNA was extracted from DMSO controls and treated *CFTR* WT and *CFTR* KO Caco2 cells. The mRNA expression levels were determined by RT-qPCR. To minimize technical variations, the expression of each gene of interest was normalized to the expression of

18S.

Interleukin-8 (IL8, CXCL8) is a cytokine that plays an important role in the recruitment of inflammatory cells and growth of colon carcinoma cell lines (Matsushima & Oppenheim, 1989; Brew *et al*., 1999). The *IL8* expression levels in *CFTR* WT and *CFTR* KO cells were analyzed. In this experiment, the *CFTR* KO cells had a higher expression of *IL8* than *CFTR* WT cells (Figure 14a). The ratio of *IL8* basal levels in *CFTR* KO cells over *CFTR* WT cells is 1.6. The data suggest that *CFTR* deficiency might enhance *IL8* expression. The expression of *IL8* was analyzed in *CFTR* WT and *CFTR* KO Caco2 cell lines treated with TG as well as in untreated controls. To determine the effect of ER stress on gene expression in each cell line, the ratio of TG treated over untreated gene expression levels was analyzed (Figure 14b). The expression levels of the *IL8* gene in both *CFTR* WT and KO cells increased after TG treatment. The *IL8* expression levels were increased 44.7 and 15.5-fold, respectively, in *CFTR* WT and *CFTR* KO cells (Figure 14b). The effect of the TG treatment on *IL8* expression in *CFTR* WT cells was more than the effect of the TG treatment on *IL8* expression in *CFTR* KO cells (Figure 14b). The difference between the expression levels in WT and KO cells after treatment is not statistically significant at $p \leq 0.05$. A trend was suggested by these data that the loss of *CFTR* causes TG to have less of an effect on *IL8* expression.

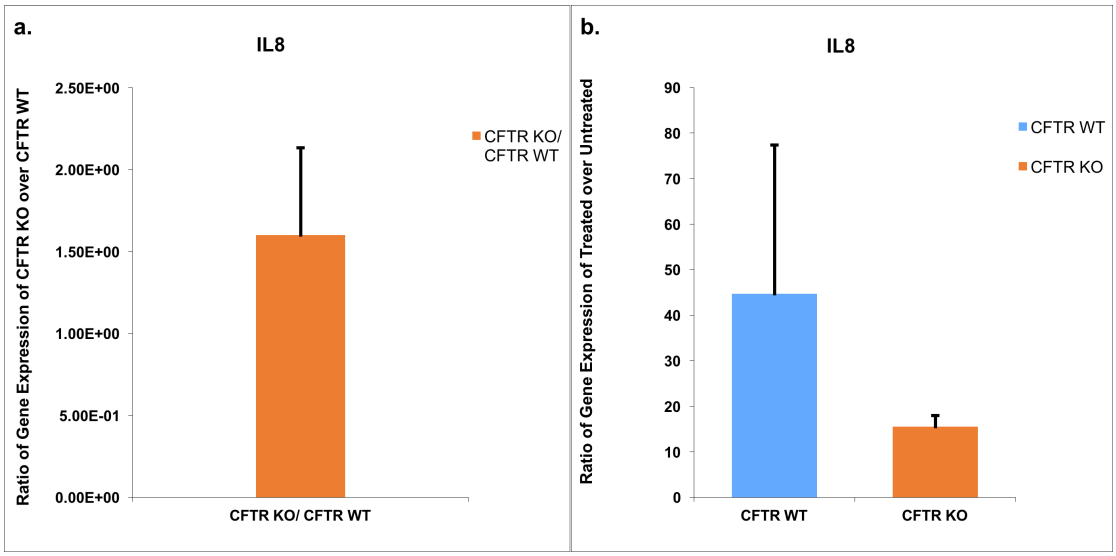

Figure 14. Expression of *IL8* in *CFTR* WT and *CFTR* KO Caco2 cell lines. *IL8* mRNA expression (a) (b) was measured by RT-qPCR. The expression of *IL8* was normalized to the expression of 18S. (a) The Y-axis refers to the ratio of *CFTR* KO cells over *CFTR* WT cells gene basal expression levels. (b) The Y-axis refers to the ratio of TG treated over untreated gene expression levels.

Tumor Necrosis Factor (*TNF*) is a cytokine involved in the regulation of inflammation, proliferation, and apoptosis (Gaur & Aggarwal, 2003). *TNF* is not only induced by NF-κB but the binding of TNF to tumor necrosis factor receptor (TNFR) also indirectly activates the NF-κB signaling pathway (Gaur & Aggarwal, 2003). The *TNF* expression levels in *CFTR* WT and *CFTR* KO cells were analyzed. In the experiment, there was no notable difference between the basal expression levels of TNF in *CFTR* WT and *CFTR* KO cells (Figure 15a). The *TNF* expression levels were analyzed in *CFTR* WT and *CFTR* KO Caco2 cell lines treated with TG as well as in untreated controls. *TNF* mRNA expression in both *CFTR* WT and KO cells increased after TG treatment. The *TNF* expression levels increased 2.3 and 1.5-fold, respectively,

in *CFTR* WT and *CFTR* KO cells (Figure 15b). The effect of the TG treatment on *TNF* expression in *CFTR* WT was more than the effect of the TG treatment on *TNF* expression in *CFTR* KO cells (Figure 15b). The difference between the expression levels in WT and KO after treatment is not statistically significant at $p \leq 0.05$. A trend was suggested by these data that the loss of *CFTR* causes TG to have less of an effect on *TNF* expression.

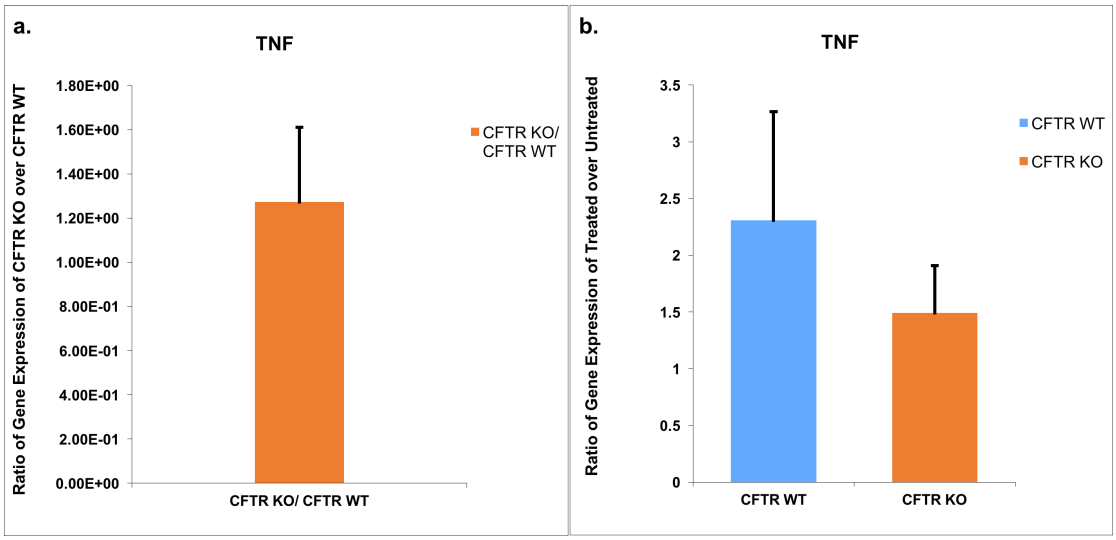

Figure 15. Expression of *TNF* in *CFTR* WT and *CFTR* KO Caco2 cell lines. *TNF* mRNA expression (a) (b) was measured by RT-qPCR. The expression of *TNF* was normalized to the expression of 18S. (a) The Y-axis refers to the ratio of *CFTR* KO cells over *CFTR* WT cells gene basal expression levels. (b) The Y-axis refers to the ratio of TG treated over untreated gene expression levels.

The *IL8* and *TNF* gene expression data consistently indicate that *CFTR* deficiency cause TG to produce less of an effect on the expression of NF-κB signaling target genes *IL8* and *TNF*. These data suggest that the loss of *CFTR* might cause TG-induced UPR to have less of an effect on NF-κB activation, but the difference is not statistically significant. More studies need to be conducted to confirm or refute this conclusion.

Discussion

The purpose of this thesis was to detect the mechanism by which *CFTR* deficiency might lead to CRC. GSEA pathway analysis suggested that *CFTR*-deficient normal and tumor tissues from mice and humans had an enriched expression in genes involved in the UPR. Altered genes, environmental stress, and increased protein synthesis induce UPR activation in cancer cells (Kaufman & Wang, 2014; Ma & Hendershot, 2004; Dejeans, Barroso, Fernandez-Zapico, Samali, Chevet, 2015). UPR has two potentially opposing effects on cancer development. On the one hand, some cancer cells need a higher level of UPR to support their growth and survival (Corazzari, Gagliardi, Fimia & Piacentini, 2017); on the other hand, increased UPR causes loss of stemness which could inhibit cancer development (Heijmans *et al*., 2013). To identify the correlation between *CFTR* deficiency and UPR activation and its effect on CRC, a pair of *CFTR* KO and WT Caco2 cell lines were utilized to test the working model that UPR activation might be enhanced in *CFTR* KO cells, and that this activation might protect CRC cell survival under ER stress. We tested the working model by observing Caco2 cell lines treated with inducers to trigger ER stress. The UPR activities were evaluated by observing mRNA expression changes of key genes. The protection from ER stress was evaluated by analyzing cell viability. These data support the hypothesis that the loss of *CFTR* increases protection from ER stress and that this protection supports the survival of CRC cells. However, the data alone does not sufficiently support my hypothesis.

RT-qPCR for *CFTR* Validates *CFTR* KO Cells

The mechanism underlying CRC suppression by *CFTR* has not been discovered. To investigate the mechanism, a pair of *CFTR* KO and *CFTR* WT Caco2 cell lines created by CRISPR-Cas9 engineering were used. Initially, the expression of *CFTR* in *CFTR* KO and *CFTR* WT cells was compared. *CFTR* is estimated to show relatively low expression in *CFTR* KO cells. RT-qPCR analysis agrees with the estimation that the expression of *CFTR* in *CFTR* KO cells is lower than in *CFTR* WT cells (Figure 5). However, *CFTR* is still expressed in RT-qPCR analysis of *CFTR* KO cells. These data suggest that *CFTR* might not be totally knocked out in *CFTR* KO Caco2 cells, even though the expression is decreased. CRISPR-Cas9 was used to induce a frameshift mutation in the exon 11 in the coding region of *CFTR* on chromosome 7 in *CFTR* KO cells, thereby knocking out *CFTR*. Theoretically, the unstable mRNA was expected to be degraded, and no CFTR protein would be produced. The primer used amplifies the DNA sequence that partly covers the 5'untranslated region (5'UTR) and partly covers a region in exon 1 on chromosome 7. It is possible that the 5'UTR and a portion of the protein-coding region accounts for the small amount seen in the knockout clone.

The question arises how *CFTR* KO cells induces UPR. We assume UPR might be activated through two different mechanisms. The first possibility is that *CFTR* mRNA with coding region might survive from degradation, as with delta 508 (Bartoszewski *et al*., 2008; Chung *et al*., 2016). In this case, the surviving partial mRNA might be translated into misfolded proteins, and the accumulation of the misfolded proteins might induce UPR. The second possible explanation is based on the biological function

of CFTR protein. CFTR is a chloride ion channel which regulates cytoplasmic chloride levels (De Lisle & Borowitz, 2013), and the uptake of Ca^{2+} into the ER lumen is important for maintaining the ER Ca^{2+} gradient (Pollock, Kargacin & Kargacin, 1998). Pollock et al. (1998) reported that chloride channel blockage suppresses Ca^{2+} uptake by Sarcoplasmic Reticulum. It is possible that the dysfunction of CFTR might impair the uptake of Ca^{2+}, and disrupted Ca^{2+} homeostasis induces ER stress (Oslowski & Urano, 2011). RT-qPCR can be used to detect what part is left in the mRNA of *CFTR* KO cells. Through designing primers amplifying the DNA sequence that covers each exon of *CFTR* coding region, we can tell which exon of *CFTR* gene is included or excluded in *CFTR* KO cells. If all exons are excluded, it may support the second possible explanation. Otherwise, the first possibility that misfolded proteins are transcribed from a portion of mRNA might account for the UPR activation in *CFTR* KO cells. Western blot could be used to identify if CFTR proteins are present. If CFTR proteins exist, these proteins might be misfolded proteins because exon 11 is depleted and the normal proteins might not be produced. If CFTR proteins are present, the first possibility might explain the UPR activation in *CFTR* KO Caco2 cell line.

CFTR **Deficiency in Caco2 Cell Lines Might Alter UPR Activation**

To detect the biological pathways affected by *CFTR* deficiency in CRC, gene expression data analyses from *CFTR*-deficient normal and tumor tissues from mice and humans were conducted through Gene Set Enrichment Analysis (GSEA). GSEA pathway analysis suggested that *CFTR*-deficient normal and tumor tissues from mice and humans were enriched in genes involved in the unfolded protein response. GSEA

offers informative suggestions, but these suggestions are not enough to draw conclusions, and analyzing gene expression in *CFTR* WT and *CFTR* KO Caco2 cell lines was necessary to help examine the UPR activities in *CFTR* KO cells. We evaluated mRNA expression changes of key genes relating to the UPR by performing RT-qPCR. The results showed no difference between the basal expression levels of *HSPA5* in *CFTR* WT and *CFTR* KO. To determine the effect of TG treatment and induction of ER stress on gene expression in each cell line, the ratio of gene expression in treated cells over untreated cells was analyzed. The expression of *HSPA5* increased after TG treatment in both *CFTR* WT and *CFTR* KO cells, which agreed with our expectation that TG-induced ER stress activates the UPR. The TG treatment had more of an effect on *HSPA5* expression in *CFTR* KO cells than on *HSPA5* expression in *CFTR* WT cells. This indicates that *CFTR* deficiency promotes the effect of TG-induced ER stress on the expression of UPR gatekeeper *HSPA5,* the common regulator for initiating three UPR sub-pathways. This is consistent with the suggestion of GSEA that the loss of *CFTR* enhances UPR activation.

No difference was found between the basal expression levels of *ATF4* in *CFTR* WT and *CFTR* KO. The expression of *ATF4* increased after treatment in both cell lines, which agreed with our expectation that TG-induced ER stress might activate UPR, especially the PERK signaling pathway. However, *ATF*4 expression increased to the same extent in both WT and KO cells, suggesting that the loss of *CFTR* might not influence the effect of TG-induced ER stress on the expression of the PERK signaling target gene *ATF4.* The RT-qPCR data of *ATF4* expression did not support our

hypothesis that *CFTR* deficiency increases the expression of UPR target genes in response to TG induced UPR. The data reflect that the loss of *CFTR* might not enhance the activation of PERK signaling.

The data of *HSPA5* and *ATF4* gene expression suggest that the loss of *CFTR* might increase UPR activities in response to ER stress but might not affect the influence of TG-induced ER stress on the expression of the PERK signaling target gene *ATF4.* Since we only tested mRNA expression levels of two genes, the conclusions we can draw from this analysis are limited. Protein expression levels need to be analyzed in order to draw more precise and accurate conclusions in the future. *ATF4* is not the only target gene of the PERK-eIF2α signaling, so analyzing the expression of other PERK signaling target genes might help evaluate the activities of this pathway more comprehensively.

In addition, Wang and Kaufman (2016) demonstrated that the three UPR sub-pathways, ATF6α, IRE1α and PERK, are not simultaneously activated by ER stress. Since we did not see an effect of *CFTR* deficiency on the specific PERK-eIF2α-ATF4 signaling, it is of interest to examine the activities of other UPR signaling branches. IRE1α plays an important role in cell fate. A study conducted by Li et al. (2017) suggests that knockdown of IRE1α suppresses tumorigenesis in colon cancer through decreasing β-catenin. The spliced *XBP1* mRNA by IRE1α activation is important for triggering adaptive functions in UPR (Hetz, Martinon, Rodriguez & Glimcher, 2011). Many studies reported that under excessive ER stress, IRE1α activation enhances *TXNIP* levels by destabilizing miR-17 (Oslowski *et al.,* 2012; Lerner *et al.,* 2012). The

increased *TXNIP* levels promote the switch from adaptive to maladaptive UPR (Oslowski *et al.,* 2012; Lerner *et al.,* 2012) and initiates apoptotic pathways (Zhao *et al.,* 2017; Lerner *et al.,* 2012; Oslowski *et al.,* 2012). To further investigate the UPR activities in *CFTR* KO cells, it is interesting to observe the expression of these two genes without artificially sustained ER stress. RT-qPCR was conducted to evaluate the expression of these two genes in *CFTR* KO and *CFTR* WT cells without TG treatment. A decrease in the expression of *XBP1* in *CFTR* KO cells suggests that the loss of *CFTR* might decrease total *XBP1* expression. The expression of spliced *XBP1* is expected to be up-regulated in *CFTR* KO cells in order to increase protein folding and cell survival. However, the total expression of *XBP1* was decreased in the *CFTR* KO cells in our experiment. This reflects that *CFTR* deficiency might not activate a specific IRE1α-XBP1 signaling pathway. It is of interest to investigate the ratio of spliced *XBP1* to unspliced *XBP1*. It is probable that the expression of spliced *XBP1* increased in *CFTR* KO cells even though the total *XBP1* expression decreased. The primer pair we used amplifies both unspliced and spliced sequences. More experiments need to be conducted to differentiate spliced *XBP1* from unspliced *XBP1* in the PCR product.

The decreased expression of *TXNIP* in *CFTR* KO cells suggests that the loss of *CFTR* might decrease *TXNIP* expression levels. Many studies reported that *TXNIP* expression is induced through the IRE1α and PERK signaling pathways (Lerner *et al.,* 2012). PERK- eIF2α phosphorylation increases the translation of ATF5 that binds to the *TXNIP* promoter and increases *TXNIP* expression (Oslowski *et al.,* 2012). Under hyperactivated irremediable ER stress IRE1α increases *TXNIP* mRNA stability by

triggering the decay of its regulator miR-17 (Lerner *et al.,* 2012). Increased *TXNIP* levels promote apoptotic pathways (Zhao *et al.,* 2017; Lerner *et al.,* 2012; Oslowski *et al.,* 2012). The down regulation of *TXNIP* in *CFTR* KO cells might provide protection from apoptosis.

Considering the two specific IRE1α pathways, the data of *XBP1* expression reflects that *CFTR* deficiency might not activate the specific IRE1α-XBP1 signaling pathway that is important for UPR adaptive functions and cell survival; the data of *TXNIP* expression suggest that the loss of *CFTR* might decrease the specific IRE1α-TXNIP pathway which initiates apoptotic pathways. The down regulation in *TXNIP* expression in *CFTR* KO cells might protect cancer cells from apoptosis. However, in these experiments, we have only tested the mRNA expression levels of these two genes without TG treatment which can induce excessive ER stress. We did not evaluate the expression of these two genes under hyperactivation of IRE1α. The conclusions we can draw from this analysis are limited. More studies need to be performed to compare the impact of *CFTR* deficiency on *TXNIP* expression under low ER stress and excessive ER stress.

To summarize, the data from these four experiments suggest that UPR activation might be up-regulated in *CFTR* KO cells, but the specific pathway might not be the one addressed in this study. In addition, the down regulation of *TXNIP* might offer protection for cancer cells from apoptosis. Except the *TXNIP*, the data of *HSPA5, ATF4* and *XBP1* genes did not show a statistically significant difference. The conclusions we can draw from these experiments are restricted. In addition to these four genes, more

analyses on the genes in the UPR need to be conducted to evaluate the UPR activities in *CFTR* WT and *CFTR* KO cells and thereby confirm or refute our conclusions.

***CFTR* Deficiency in Caco2 Might Offer Protection Against Excessive ER Stress**

Although many cancer cells need high UPR to support them, excessive prolonged activation triggers a switch to an apoptotic pathway (Wang & Kaufman, 2016; Niederreiter, L. *et al.,* 2013). To detect if the loss of *CFTR* protects the survival of CRC under hyperactivated irremediable ER stress, we compared cell viability of *CFTR* KO and WT cells under ER stress. The MTT assay was performed to determine the cell viability of *CFTR* KO and WT cells treated with TG to trigger ER stress. The initial step was to compare the cell viability of *CFTR* WT and *CFTR* KO Caco2 cell lines before TG treatment. The results showed that without TG treatment, *CFTR* WT cells had a slightly higher cell viability over the duration of plating (Figure 10). These data reflect the differences in cell growth between *CFTR* WT and *CFTR* KO cells and it occurred in all of our MTT experiments.

After treatment, the cell viability changes after the induction of ER stress in *CFTR* WT and KO cells were determined with the use of the MTT assay. For analysis, MTT values at each point were normalized to 3h untreated controls for *CFTR* WT and *CFTR* KO cells to control the differences between plating. The result showed decreased cell viability after treatment in both *CFTR* WT and *CFTR* KO cells, which agreed with our expectation that TG induced ER stress might impair cell viability. To identify the effect of TG-induced ER stress on each cell line, the ratio of treated over untreated viability at each point was analyzed. The data showed a higher ratio in *CFTR* KO cells, indicating

that the loss of *CFTR* might cause TG-induced ER stress to have less of an effect on cell viability. These data agreed with our expectation that *CFTR* deficiency might relieve the effect of ER stress on viability. This suggests that the loss of *CFTR* might promote protection of colon cancer from excessive ER stress.

To test the influence of *CFTR* deficiency, the cell viability changes in *CFTR* WT and KO cells after the induction of ER stress by another inducer, Tunicamycin (TM), was determined by conducting the MTT assay. The results showed declined cell viability after TM treatment in both *CFTR* WT and *CFTR* KO cells. This result agreed with our expectation that TM-induced ER stress might impair cell viability. To identify the effect of TM-induced ER stress on each cell line, the ratio of treated over untreated viability at each point was analyzed. The result showed that *CFTR* KO cells were less affected by TM treatment than WT cells. This indicates that the loss of *CFTR* might cause TM-induced ER stress to have less of an effect on cell viability. Only one biological replicate was evaluated in this experiment. More biological replicates and experiments are needed to confirm or refute this result. Both TG treatment and TM treatment experiments showed that the cell viability of *CFTR* KO cells was less impaired by ER stress than that of WT cells. These data agreed with our hypothesis that the loss of *CFTR* deficiency might protect the survival of CRC cells from excessive ER stress.

The previous experiment showed decreased *TXNIP* expression in *CFTR* KO cells. Many studies reported that increased *TXNIP* expression levels lead to apoptosis (Oslowski *et al.,* 2012; Lerner et al., 2012). Besides, a previous member of our lab, Dr.

Lei Zhao, showed the inhibiting role of *TXNIP* in cell viability in another CRC cell line, SW480 (Zhao, 2013). It is probable that the decreased *TXNIP* levels caused by *CFTR* deficiency relieves the effect of *TXNIP* on the initiation of apoptosis, and this relief might protect the survival of CRC cells. However, the experiments and analyses in this thesis are not enough to draw conclusions on this. More studies are required to test the correlation between *CFTR*, *TXNIP* and CRC cell survival.

CFTR **Deficiency in Caco2 Cell Lines Appeared to Restrict Activation of NF-κB in Response to UPR**

Grootjans et al. (2016) demonstrated that ER stress induced UPR triggers NF-κB activation. Recent research reported that *CFTR* deficiency activates the NF-κB signaling pathway (Crites *et al*., 2015). We hypothesized that *CFTR* deficiency might enhance NF-κB activation in the presence of UPR. To observe NF-κB activity in *CFTR* KO cells in response to UPR, RT-qPCR analysis was performed to compare the gene expression changes relating to the NF-κB signaling pathway in *CFTR* WT and *CFTR* KO Caco2 cell lines treated with TG to trigger ER stress. The result showed increased *IL8* basal expression levels in *CFTR* KO cells, suggesting that *CFTR* deficiency might enhance the expression of the NF-κB target gene *IL8*. These data were consistent with microarray and IPA analyses in mice performed by Than et al. (2016). That study found the enrichment of gene sets involved in the immune response in *Cftr*- deficient tumors and normal tissues acquired from colons and small intestines. It is of interest to investigate the correlation between the NF-κB signaling pathway and *CFTR* in CRC.

The conclusion drawn from the mRNA expression of one gene is limited, and the results need to be confirmed by more studies.

To determine the effect of TG treatment and induction of UPR on gene expression in *CFTR* WT and *CFTR* KO cells, the ratio of gene expression in treated cells over untreated cells was analyzed. The results showed increased expression of *IL8* after treatment in both *CFTR* WT and *CFTR* KO cells, which agreed with our expectation that ER stress induced UPR might activate NF-κB signaling. The treatment had less of an effect on *IL8* expression in *CFTR* KO. These data indicate that *CFTR* deficiency might cause TG to have less of an effect on *IL8* expression. Instead, this result was not expected. We hypothesized that the loss of *CFTR* might enhance the activation of the NF-κB signaling pathway in response to UPR.

Surprisingly, the result of RT-qPCR showed no difference between the *TNF* basal expression levels in *CFTR* WT and *CFTR* KO. This result is not consistent with our expectation that *CFTR* deficiency activates the NF-κB signaling pathway. It is possible that the mRNA stability of *TNF* might be low in *CFTR* KO and the low mRNA stability might negatively affect the expression level, because previous studies state that the expression of TNF mRNA is regulated at a transcriptional level and a posttranscriptional level including mRNA stability and polyadenylation (Szlosarek, et al., 2006; Anderson, 2000).

After TG treatment, the results showed increased expression of *TNF* in both cell lines, which was consistent with our expectation that ER stress induced UPR might trigger NF-κB activation. The TG treatment had less of an effect on the expression of

TNF mRNA in *CFTR* KO cells. This suggests that defective *CFTR* might cause TG to have less of an effect on *TNF* expression. This result was not expected but similar to the effect of TG treatment on *IL8* expression in *CFTR* KO cells. These data of *IL8* and *TNF* mRNA expression consistently suggest that *CFTR* deficiency might cause TG to produce less of an effect on the expression of NF-κB signaling target genes *IL8* and *TNF*. The data suggest that *CFTR* deficiency might cause TG-induced UPR to have less of an effect on NF-κB activation. In this experiment, we only tested mRNA expression levels of two genes relating to NF-κB, and the conclusions we can draw from this analysis are limited. The expression of other genes associated with NF-κB need to be tested in order to draw more precise and accurate conclusions in the future. Supervising the specific pathways through which UPR activates NF-κB signaling, like IRE1α and PERK, might help to explain why the TG treatment has less of an effect on the expression of *TNF* mRNA in *CFTR* KO.

Vlantis et al. (2016) reported that enhanced activation of NF-κB in the intestinal epithelium promotes cell proliferation and offers a tumor-promoting microenvironment, contributing to the intestinal tumorigenesis. *IL8* plays an important role in the recruitment of inflammatory cells and growth of colon carcinoma cell lines (Matsushima & Oppenheim, 1989; Brew *et al*., 1999). The enhanced expression of the NF-κB target gene *IL8* in *CFTR* KO might suggest an increased activation of NF-κB signaling in *CFTR* KO and this activation might support the growth of cancer cells. The expression of other genes relating to NF-κB signaling needs to be tested in order to draw more precise and accurate conclusions in the future.

Conclusion and Future Directions

Our data suggest that *CFTR* deficiency might enhance UPR activation even though the specific pathway might not be the one addressed in this study, and that the down regulation of *TNXIP* might offer protection for CRC cell survival. Considering the two possible roles of the UPR on CRC, one is that a higher level of UPR supports survival of some cancer cells (Corazzari, Gagliardi, Fimia & Piacentini, 2017); the other one is that increased UPR causes the differentiation of stem cells which could inhibit cancer development (Heijmans *et al*., 2013). Our data support the first possibility or suggest that the cancer supporting effect is stronger. Caco2 is a colon cancer cell line and it has a heterogeneous population of cancer cells. Its oncogenic potential is different from that of untransformed stem cells and thus, Caco2 might not be a good model to test if enhanced UPR activation suppresses cancer development through inducing the differentiation of stem cells. It is of interest to evaluate if *CFTR* deficiency activates UPR and if *CFTR* deficiency activated UPR supports CRC cell survival in models which have normal numbers of intestinal stem cells.

Our data did not support our hypothesis that *CFTR* deficiency positively affects the NF-κB signaling pathway in the presence of UPR. It is of interest to perform more studies to characterize the relationship between *CFTR* and the NF-κB pathway in response to UPR in CRC. For example, the ER Stress TF Activation Profiling Plate Array can be utilized to simultaneously monitor ER stress and UPR related transcription factors, including NF-κB, ATF4, ATF6, CHOP, AP-1and p53. The data that enhanced basal expression levels of the NF-κB target gene *IL8* in *CFTR* KO cells

might suggest an increased activation of NF-κB signaling in *CFTR* KO cells and this activation might support the growth of cancer cells.

Considering the gene expression data and cell viability analysis data, we draw the conclusion that in Caco2 CRC cells *CFTR* deficiency may alter the response to UPR in several pathways, which may promote cancer cell survival. Additional experiments must be done to determine which ones among these altered pathways are vital for cancer development. Our data support our working model that UPR activation might be enhanced in *CFTR* KO, and this activation might protect CRC cell survival under ER stress. These data might contribute to investigating the relation between UPR and the cancer supporting effects of *CFTR*-deficiency. The findings of this thesis offer potential insights into the mechanism underlying CRC suppression by *CFTR*. This knowledge might help in therapies for CRC.

There are limitations in this study, and more studies need to be conducted to completely support our hypothesis. In the future, mRNA expression and protein expression levels of more genes involved in the three UPR sub-pathways and NF-κB signaling should be evaluated. Different types of inducers should be used to evaluate cell viability in the presence of ER stress in combination with varying nutrition conditions. Other colon cancer cell lines, normal colon cell lines and tissue culture methods are suggested to be used in order to examine the relation between *CFTR* deficiency and UPR activation and their effects on CRC. More biological replicates are required, and these data might confirm our working model.

Material and Methods

Cell Culture and Treatment

CFTR WT and *CFTR* KO Caco2 cell lines were provided by Mitchell Drumm from Case Western Reserve University and cultured in a culture medium composed of EMEM (Mediatech, 639688), 10% fetal bovine serum (FBS) and L- Glutamine (Mediatech, 21716002). The cells were cultured in 100mm tissue culture dishes at 37°C in a humidified atmosphere of 5% CO2.

To compare the mRNA expression of genes in *CFTR* WT cells and *CFTR* KO cells, total RNA was extracted from *CFTR* WT and *CFTR* KO Caco2 cells. One million (10^6) cells were plated in 100mm tissue culture dishes and grown for 18 hours at 37°C. RT-qPCR was conducted to test mRNA expression levels.

For the Thapsigargin (TG) treatment study, the cells were grown in EMEM and put into four groups: the *CFTR* WT cells control group, incubation with 0.1% DMSO; the *CFTR* WT cells treatment group, incubation with 0.2 μM TG; the *CFTR* KO cells control group, incubation with 0.1% DMSO; the *CFTR* KO cells treatment group, incubation with 0.2 μM TG. To prepare for RNA extraction, one million (10^6) cells were plated in 100 mm tissue culture dishes and grown for 18 hours at 37°C before treatment. Cells were treated with 0.2 μM TG for 2.5 hours, then RNA were acquired. RT-qPCR was conducted to test mRNA expression levels.

To compare cell viability of *CFTR* WT and *CFTR* KO Caco2 cell lines, cells were prepared for the MTT assay. Twenty-five hundred (2,500) Caco2 cells per well, 5,000 Caco2 cells per well, and 10,000 Caco2 cells per well with 6 technical replicates were

plated into a 96-well plate and cultured from 18 hours to 90 hours in 1 biological replicate. The MTT assay was conducted to test cell viability.

For the dose gradient of the TG treatment study, cells were prepared for MTT assay. Ten thousand (10,000) Caco2 cells per well with 6 technical replicates were plated into a 96-well plate and grown for 18 hours at 37°C before treatment. The cells were treated with the TG with different doses (0.2 μM, 0.4 μM, 0.8 μM) over time, at 2 hours, 24 hours, 48 hours, and 72 hours in 1 biological replicate. The MTT assay was conducted to test cell viability after the TG treatment at the same intervals.

To compare cell viability of *CFTR* WT and *CFTR* KO Caco2 cell lines under ER stress, cells were prepared for the MTT assay. Five thousand (5,000) Caco2 cells per well with 6 technical replicates were plated into a 96-well plate and grown for 18 hours at 37°C before treatment. The cells were treated with the 0.2 μM TG over time, at 3 hours, 24 hours, 48 hours, and 72 hours in 3 biological replicates. The MTT assay was conducted to test cell viability after the TG treatment at the same intervals.

For the Tunicamycin (TM) treatment study, the cells were grown in EMEM and put into four groups: the *CFTR* WT cells control group, incubation with 0.1% DMSO; the *CFTR* WT cells treatment group, incubation with 2.5 μg/ml TM, incubation with 5 μg/ml TM, incubation with 10 μg/ml TM; the *CFTR* KO cells control group, incubation with 0.1% DMSO; the *CFTR* KO cells treatment group, incubation with 2.5 μg/ml TM, incubation with 5 μg/ml TM, incubation with 10 μg/ml TM. To compare cell viability of *CFTR* WT and *CFTR* KO Caco2 cell lines under ER stress, cells were prepared for the MTT assay. Twenty thousand (20,000) Caco2 cells per well with 6

technical replicates were plated into a 96-well plate, and grown for 18 h at 37°C before treatment. The cells were treated with the TM with different doses (2.5 µg/ml, 5 µg/ml, 10 µg/ml) over time, at 2 hours, 24 hours, 48 hours, and 72 hours in 1 biological replicate. The MTT assay was conducted to test cell viability after the TM treatment at the same intervals.

RNA Extraction

Total cellular RNA was isolated using a Qiagen RNeasy Mini Kit (Qiagen, Hilden, Germany), according to the manufacturer's recommendations. RNA concentration was calculated based on the absorbance at 260nm. RNA samples were stored at −20°C.

Quantitative Reverse Transcriptase Polymerase Chain Reaction (RT- qPCR)

The standard cDNA was reverse-transcribed from 1.5µg of total RNA from the T84 colon cancer cell line using a Qiagen Omniscript RT Kit (cat. No. 205113) and the specific primer.

The total cDNA was reverse-transcribed from 1.5 µg of total RNA from *CFTR* WT *and CFTR* KO Caco2 cell lines using a Qiagen Omniscript RT Kit (cat. No. 205113) and Random Primer 9.

Quantitative polymerase chain reaction (qPCR) monitors the amplification of target DNA during the PCR in real-time using fluorescent dyes which bind non-specifically to double stranded DNA. The PCR products can be detected by measurement of SYBR Green I fluorescence signals. SYBR Green I binds to the double stranded DNA helix. The SYBR Green I fluorescence signal is proportional to the

amount of double-stranded DNA produced by PCR. The computer linked to the Roche Light Cycler 480 Real-Time PCR Instrument would produce an amplification curve which displays the fluorescence values versus cycle number. The threshold of the amplification curve reflects a significant increase over the initial cycles of PCR. The cycle number at which the fluorescent signal of the reaction crosses the threshold is defined as threshold cycle (C_t), which is used to calculate the initial DNA copy number, because the C_t value is inversely related to the starting amount of a sample. The 5-point, 10-fold serial dilution of the target standard would have 5 curves on a plot and thus have 5 C_t values. Then the computer would generate a standard curve which reflects the relationship between the starting quantity (X axis) which is already known and C_t values (Y axis) for each target gene or 18S. To measure the level of expression of a gene in a new sample, qPCR was performed to this sample and standards. The sample will have a C_t value after amplification, and the starting quantity of the sample will be calculated by comparison with the standard curve for each target gene or 18S.

The standard cDNA was amplified with the use of the Qiagen HotStarTaq Master Mix Kit (cat. No. 203443) and then purified with the use of the Qiagen MinElute PCR Purification Kit (cat. No. 28004). The concentration of purified amplified cDNA was determined by using the Nanodrop 2000 spectrophotometer (NanoDrop, ThermoScientific). After calculation, the purified amplified cDNA was diluted to a standard stock at 5E9 copies/µl in order to prepare a 5-point, 10-fold serial dilution of the target standard. A 5-point standard curve was set up: E7 copies/µl to E2 copies/µl.

The total cDNA was amplified with the use of the Qiagen HotStarTaq Master Mix

Kit (cat. No. 203443). The 1: 10 dilutions of concentrated cDNA and 1: 100 dilutions of concentrated cDNA were prepared. A standard curve composed of ten-fold serial dilutions of concentrated cDNA was included in each qPCR run for each specific target primer. A standard curve composed of 1: 100 dilutions of concentrated cDNA was included in each qPCR run for the 18S primer. The input of 15 ng total cDNA in duplicate per sample was used for each specific target primer pair, and the input of 1.5 ng cDNA in duplicate per sample was used for each 18S primer pair. The expression level of each target gene or 18S in cDNA was calculated based on the standard curve of PCR amplification for each target gene or 18S. Reactions were performed with the use of a SYBR Green I Master Kit and 10 µM of each primer per reaction in a total volume of 20 µl on the Roche Light Cycler 480 Real-Time PCR Instrument. The reactions include: pre-incubation at 95°C for five minutes in one cycle; amplification- 45 cycles, 95°C for five seconds, 60°C for five seconds, and 72°C for ten seconds; melting curve- 1cycle, 95°C for five seconds, 65°C for one minute, and 97°C in continuous mode; cooling- 1 cycle, until 40°C for thirty seconds. Expression of each specific target gene was normalized to 18S and expressed as a fold induction.

List of primers used

All primers were designed using Primer-BLAST (National Center for Biotechnology Information) and obtained from Integrated DNA Technologies (Coralville, IA, USA).

Gene	Primer	Sequence (5'- 3')
XBP1	Forward primer	GGGGAATGAAGTGAGGCCAG
	Reverse primer	TTGTCCAGAATGCCCAACAGG
TXNIP	Forward primer	TTCGGAGTACCTGCGCTATG
	Reverse primer	AGGAAGCTCAAAGCCGAACT
ATF4	Forward primer	AGGAGGAAGACACCCCTTCA
	Reverse primer	ATCGTAAGGTTTGGGACGGG
HSPA5	Forward primer	GAACGTCTGATTGGCGATGC
	Reverse primer	TCAACCACCTTGAACGGCAA
CFTR	Forward primer	GACATCACAGCAGGTCAGAGAA
	Reverse primer	CAACGCTGGCCTTTTCCAGA
18S	Forward primer	CGCCGCTAGAGGTGAAATTCTT
	Reverse primer	CAGTCGGCATCGTTTATGGTC

IL8	Forward primer	ACCGGAAGGAACCATCTCAC
	Reverse primer	AAACTGCACCTTCACACAGAG
TNF	Forward primer	GCTGCACTTTGGAGTGATCG
	Reverse primer	GAGGGTTTGCTACAACATGGG

MTT Assay

The MTT assay is a colorimetric assay that measures the conversion of the yellow color MTT into purple formazan via the mitochondrial enzyme succinate dehydrogenase in live cells (Mosmann, 1983). The prepared cells were grown in EMEM and incubated with 0.1% DMSO or treated with ER stress inducers over time. Then the medium was replaced with EMEM and supplemented with 0.5 mg/ml MTT Reagent. After 4 hours of incubation, the purple formazan crystals within the live cells were dissolved in 100 µl SDS in each well. The extent of color conversion is quantitated by measuring absorbance in a plate reader at wavelength of 590 nm. Wells without cells were used as blanks and were subtracted as background from each sample.

Statistical Analysis

All quantitative results are given as averages with standard deviation unless otherwise stated. A paired two-tailed *t*-test was used to determine the statistical significance of the entirety of the RT-qPCR data and MTT data in this thesis. All

statistical tests used a significance value of $\alpha = 0.05$. Comparisons of $p \leq 0.05$ are marked by an asterisk *. The p values are not shown in the results when $p > 0.05$.

References

1. Lee, K., Tirasophon, W., Shen, X., Michalak, M., Prywes, R., Okada, T., … Kaufman, R. J. (2002). IRE1-mediated unconventional mRNA splicing and S2P-mediated ATF6 cleavage merge to regulate XBP1 in signaling the unfolded protein response. *Genes & Development*, *16*(4), 452–466.
2. Anderson, P. (2000). Post-transcriptional regulation of tumour necrosis factor α production. *Annals of the Rheumatic Diseases*, *59*(Suppl 1), i3–i5.
3. Barker, N., Ridgway, R. A., van Es, J. H., van de Wetering, M., Begthel, H., van den Born, M., … Clevers, H. (2009). Crypt stem cells as the cells-of-origin of intestinal cancer. *Nature*, *457*(7229), 608–611.
4. Barker, N., van Es, J. H., Kuipers, J., Kujala, P., van den Born, M., Cozijnsen, M., … Clevers, H. (2007). Identification of stem cells in small intestine and colon by marker gene Lgr5. *Nature*, *449*(7165), 1003–1007.
5. Bartoszewski, R., Rab, A., Jurkuvenaite, A., Mazur, M., Wakefield, J., Collawn, J. F., & Bebők, Z. (2008). Activation of the unfolded protein response by ΔF508 CFTR. *American Journal of Respiratory Cell and Molecular Biology*, *39*(4), 448.
6. Billings, J. L., Dunitz, J. M., McAllister, S., Herzog, T., Bobr, A., & Khoruts, A. (2014). Early colon screening of adult patients with cystic fibrosis reveals high incidence of adenomatous colon polyps: *Journal of Clinical Gastroenterology*, *48*(9), e85–e88.
7. Borchardt, R. T. (2011). Hidalgo, I. J., Raub, T. J., and Borchardt, R. T.: Characterization of the human colon carcinoma cell line (Caco-2) as a model system for intestinal epithelial permeability, Gastroenterology, 96, 736–749, 1989—The Backstory. *The AAPS Journal*, *13*(3), 323–327.
8. Brannon, A. R., Vakiani, E., Sylvester, B. E., Scott, S. N., McDermott, G., Shah, R. H., … Berger, M. F. (2014). Comparative sequencing analysis reveals high genomic concordance between matched primary and metastatic colorectal cancer lesions. *Genome Biology*, *15*(8), 454.
9. Brew, R., Erikson, J. S., West, D. C., Kinsella, A. R., Slavin, J., & Christmas, S. E. (2000). Interleukin-8 as an autocrine growth factor for human colon carcinoma cells in vitro. *Cytokine*, *12*(1), 78–85.
10. Brew, Robert, Erikson, J. S., West, D. C., Kinsella, A. R., Slavin, J., & Christmas, S. E. (2000). Interleukin-8 as an autocrine growth factor for human colon carcinoma cells in vitro. *Cytokine*, *12*(1), 78–85.
11. Broad Institute. (2018, January). GSEA Overview. Retrieved March 16, 2018, from http://software.broadinstitute.org/gsea/index.jsp
12. Calabrese, P., Mecklin, J.-P., Järvinen, H. J., Aaltonen, L. A., Tavaré, S., & Shibata, D. (2005). Numbers of mutations to different types of colorectal cancer. *BMC Cancer*, *5*, 126.
13. Cavallo, R. A., Cox, R. T., Moline, M. M., Roose, J., Polevoy, G. A., Clevers, H., … Bejsovec, A. (1998). *Drosophila* Tcf and Groucho interact to repress Wingless signalling activity. *Nature*, *395*(6702), 604–608.

14. Chevet, E., Hetz, C., & Samali, A. (2015). Endoplasmic reticulum stress-activated cell reprogramming in oncogenesis. *Cancer Discovery*, *5*(6), 586–597.
15. Chung, W. Y., Song, M., Park, J., Namkung, W., Lee, J., Kim, H., … Kim, J. Y. (2016). Generation of ΔF508-CFTR T84 cell lines by CRISPR/Cas9-mediated genome editing. *Biotechnology Letters*, *38*(12), 2023–2034.
16. Clevers, H. (2013). The intestinal crypt, a prototype stem cell compartment. *Cell*, *154*(2), 274–284.
17. Clevers, H., & Nusse, R. (2012). Wnt/β-Catenin signaling and disease. *Cell*, *149*(6), 1192–1205.
18. Corazzari, M., Gagliardi, M., Fimia, G. M., & Piacentini, M. (2017). Endoplasmic reticulum stress, unfolded protein response, and cancer cell fate. *Frontiers in Oncology*, *7*.
19. Crites, K. S.-M., Morin, G., Orlando, V., Patey, N., Cantin, C., Martel, J., … Mailhot, G. (2015). CFTR Knockdown induces proinflammatory changes in intestinal epithelial cells. *Journal of Inflammation*, *12*, 62.
20. De Lisle, R. C., & Borowitz, D. (2013). The cystic fibrosis intestine. *Cold Spring Harbor Perspectives in Medicine*, *3*(9).
21. De Rosa, M., Pace, U., Rega, D., Costabile, V., Duraturo, F., Izzo, P., & Delrio, P. (2015). Genetics, diagnosis and management of colorectal cancer (Review). *Oncology Reports*, *34*(3), 1087–1096.
22. Dejeans, N., Barroso, K., Fernandez-Zapico, M. E., Samali, A., & Chevet, E. (2015). Novel roles of the unfolded protein response in the control of tumor development and aggressiveness. *Seminars in Cancer Biology*, *33*, 67–73.
23. Dow, L. E., O'Rourke, K. P., Simon, J., Tschaharganeh, D. F., van Es, J. H., Clevers, H., & Lowe, S. W. (2015). Apc Restoration Promotes Cellular Differentiation and Reestablishes Crypt Homeostasis in Colorectal Cancer. *Cell*, *161*(7), 1539–1552.
24. Fearon, E. R. (2011). Molecular Genetics of Colorectal Cancer. *Annual Review of Pathology: Mechanisms of Disease*, *6*(1), 479–507.
25. Fearon, E. R., & Vogelstein, B. (1990). A genetic model for colorectal tumorigenesis. *Cell*, *61*(5), 759–767.
26. Gaur, U., & Aggarwal, B. B. (2003). Regulation of proliferation, survival and apoptosis by members of the TNF superfamily. *Biochemical Pharmacology*, *66*(8), 1403–1408.
27. Govindarajan, R., Duraiyan, J., Kaliyappan, K., & Palanisamy, M. (2012). Microarray and its applications. *Journal of Pharmacy & Bioallied Sciences*, *4*(Suppl 2), S310–S312.
28. Grootjans, J., Kaser, A., Kaufman, R. J., & Blumberg, R. S. (2016). The unfolded protein response in immunity and inflammation. *Nature Reviews. Immunology*, *16*(8), 469–484.
29. Hanahan, D., & Weinberg, R. A. (2011). Hallmarks of cancer: the next generation. Cell, 144(5), 646–674.

30. Heath, J. K. (2010). Transcriptional networks and signaling pathways that govern vertebrate intestinal development. In *Current Topics in Developmental Biology* (Vol. 90, pp. 159–192). Elsevier.
31. Hedegaard, J., Arce, C., Bicciato, S., Bonnet, A., Buitenhuis, B., Collado-Romero, M., … Watson, M. (2009). Methods for interpreting lists of affected genes obtained in a DNA microarray experiment. *BMC Proceedings*, *3*(Suppl 4), S5.
32. Heijmans, J., van Lidth de Jeude, J. F., Koo, B.-K., Rosekrans, S. L., Wielenga, M. C. B., van de Wetering, M., … van den Brink, G. R. (2013). ER stress causes rapid loss of intestinal epithelial stemness through activation of the unfolded protein response. *Cell Reports*, *3*(4), 1128–1139.
33. Hetz, C. (2012). The unfolded protein response: controlling cell fate decisions under ER stress and beyond. *Nature Reviews Molecular Cell Biology*, *13*(2), 89–102.
34. Hetz, C., Martinon, F., Rodriguez, D., & Glimcher, L. H. (2011). The unfolded protein response: integrating stress signals through the stress sensor IRE1α. *Physiological Reviews*, *91*(4), 1219–1243.
35. Hu, P., Han, Z., Couvillon, A. D., Kaufman, R. J., & Exton, J. H. (2006). Autocrine tumor necrosis factor alpha links endoplasmic reticulum stress to the membrane death receptor pathway through IRE1alpha-mediated NF-kappaB activation and down-regulation of TRAF2 expression. *Molecular and Cellular Biology*, *26*(8), 3071–3084.
36. Jiménez-Marín, Á., Collado-Romero, M., Ramirez-Boo, M., Arce, C., & Garrido, J. J. (2009). Biological pathway analysis by ArrayUnlock and Ingenuity Pathway Analysis. *BMC Proceedings*, *3*(Suppl 4), S6.
37. Kaser, A., & Blumberg, R. S. (2009). Endoplasmic reticulum stress in the intestinal epithelium and inflammatory bowel disease. *Seminars in Immunology*, *21*(3), 156–163.
38. Kaser, A., Flak, M. B., Tomczak, M. F., & Blumberg, R. S. (2011). The unfolded protein response and its role in intestinal homeostasis and inflammation. *Experimental Cell Research*, *317*(19), 2772–2779.
39. Kaser, A., Lee, A.-H., Franke, A., Glickman, J. N., Zeissig, S., Tilg, H., … Blumberg, R. S. (2008). XBP1 links ER stress to intestinal inflammation and confers genetic risk for human inflammatory bowel disease. *Cell*, *134*(5), 743–756.
40. Khalek, F. J. A., Gallicano, G. I., & Mishra, L. (2010). Colon cancer stem cells. *Gastrointestinal Cancer Research : GCR*, (Suppl 1), S16–S23.
41. Kinzler, K. W., & Vogelstein, B. (1996). Lessons from hereditary colorectal cancer. *Cell*, *87*(2), 159–170.
42. Lerner, A. G., Upton, J.-P., Praveen, P. V. K., Ghosh, R., Nakagawa, Y., Igbaria, A., … Papa, F. R. (2012). IRE1α induces thioredoxin-interacting protein to activate the NLRP3 inflammasome and promote programmed cell death during endoplasmic reticulum stress. *Cell Metabolism*, *16*(2), 250–264.

43. Li, V. S. W., Ng, S. S., Boersema, P. J., Low, T. Y., Karthaus, W. R., Gerlach, J. P., … Clevers, H. (2012). Wnt Signaling through Inhibition of β-Catenin Degradation in an Intact Axin1 Complex. *Cell*, *149*(6), 1245–1256.
44. Li, X.-X., Zhang, H.-S., Xu, Y.-M., Zhang, R.-J., Chen, Y., Fan, L., … Fang, J. (2017). Knockdown of IRE1α inhibits colonic tumorigenesis through decreasing β-catenin and IRE1α targeting suppresses colon cancer cells. *Oncogene*, *36*(48), 6738–6746.
45. Ma, Y., & Hendershot, L. M. (2004). The role of the unfolded protein response in tumour development: friend or foe? *Nature Reviews. Cancer*, *4*(12), 966–977.
46. Maisonneuve, P., Marshall, B. C., Knapp, E. A., & Lowenfels, A. B. (2013). Cancer Risk in Cystic Fibrosis: A 20-year nationwide study from the United States. *JNCI: Journal of the National Cancer Institute*, *105*(2), 122–129.
47. Martin, T. A., Ye, L., Sanders, A. J., Lane, J., & Jiang, W. G. (2013). Cancer invasion and metastasis: molecular and cellular perspective. *Landes Bioscience.*
48. Matsushima, K., & Oppenheim, J. J. (1989). Interleukin 8 and MCAF: novel inflammatory cytokines inducible by IL 1 and TNF. *Cytokine*, *1*(1), 2–13.
49. Moser, A. R., Mattes, E. M., Dove, W. F., Lindstrom, M. J., Haag, J. D., & Gould, M. N. (1993). ApcMin, a mutation in the murine Apc gene, predisposes to mammary carcinomas and focal alveolar hyperplasias. *Proceedings of the National Academy of Sciences of the United States of America*, *90*(19), 8977–8981.
50. Mosmann, T. (1983). Rapid colorimetric assay for cellular growth and survival: Application to proliferation and cytotoxicity assays. *Journal of Immunological Methods*, *65*(1–2), 55–63.
51. Niccum, D. E., Billings, J. L., Dunitz, J. M., & Khoruts, A. (2016). Colonoscopic screening shows increased early incidence and progression of adenomas in cystic fibrosis. *Journal of Cystic Fibrosis*, *15*(4), 548–553.
52. Niederreiter, L., Fritz, T. M. J., Adolph, T. E., Krismer, A.-M., Offner, F. A., Tschurtschenthaler, M., … Kaser, A. (2013). ER stress transcription factor Xbp1 suppresses intestinal tumorigenesis and directs intestinal stem cells. *Journal of Experimental Medicine*, *210*(10), 2041–2056.
53. Oslowski, C. M., Hara, T., O'Sullivan-Murphy, B., Kanekura, K., Lu, S., Hara, M., … Urano, F. (2012). Thioredoxin-interacting protein mediates ER stress-induced β cell death through initiation of the inflammasome. *Cell Metabolism*, *16*(2), 265–273.
54. Oslowski, C. M., & Urano, F. (2011). Measuring ER stress and the unfolded protein response using mammalian tissue culture system. *Methods in Enzymology*, *490*, 71–92.
55. Parker, M. M., Chase, R. P., Lamb, A., Reyes, A., Saferali, A., Yun, J. H., … Castaldi, P. J. (2017). RNA sequencing identifies novel non-coding RNA and exon-specific effects associated with cigarette smoking. *BMC Medical Genomics*, *10*(1).

56. Pollock, N. S., Kargacin, M. E., & Kargacin, G. J. (1998). Chloride channel blockers inhibit Ca2+ uptake by the smooth muscle sarcoplasmic reticulum. *Biophysical Journal*, *75*(4), 1759–1766.
57. Rozpędek, W., Pytel, D., Mucha, B., Leszczyńska, H., Diehl, J. A., & Majsterek, I. (2016). The role of the PERK/eIF2α/ATF4/CHOP signaling pathway in tumor progression during endoplasmic reticulum stress. *Current Molecular Medicine*, *16*(6), 533–544.
58. Schröder, M., & Kaufman, R. J. (2005). The Mammalian Unfolded Protein Response. *Annual Review of Biochemistry*, *74*(1), 739–789.
59. Sood, R., Bear, C., Auerbach, W., Reyes, E., Jensen, T., Kartner, N., … Buchwald, M. (1992). Regulation of CFTR expression and function during differentiation of intestinal epithelial cells. *The EMBO Journal*, *11*(7), 2487–2494.
60. Starr, T. K., Allaei, R., Silverstein, K. A. T., Staggs, R. A., Sarver, A. L., Bergemann, T. L., … Largaespada, D. A. (2009). A transposon-based genetic screen in mice identifies genes altered in colorectal cancer. *Science*, *323*(5922), 1747–1750.
61. Starr, T. K., Scott, P. M., Marsh, B. M., Zhao, L., Than, B. L. N., O'Sullivan, M. G., … Cormier, R. T. (2011). A Sleeping Beauty transposon-mediated screen identifies murine susceptibility genes for adenomatous polyposis coli (Apc)-dependent intestinal tumorigenesis. *Proceedings of the National Academy of Sciences*, *108*(14), 5765–5770.
62. Szlosarek, P. W., Grimshaw, M. J., Kulbe, H., Wilson, J. L., Wilbanks, G. D., Burke, F., & Balkwill, F. R. (2006). Expression and regulation of tumor necrosis factor alpha in normal and malignant ovarian epithelium. *Molecular Cancer Therapeutics*, *5*(2), 382–390.
63. Than, B., Linnekamp, J., Starr, T., Largaespada, D., Rod, A., Zhang, Y., … Cormier, R. (2016). CFTR is a tumor suppressor gene in murine and human intestinal cancer. *Oncogene*, *35*(32), 4179–4187.
64. The American Cancer Society. Key Statistics for Colorectal Cancer. Retrieved February 9, 2018, from https://www.cancer.org/cancer/colon-rectal-cancer/about/key-statistics.html
65. Urano, F., Wang, X., Bertolotti, A., Zhang, Y., Chung, P., Harding, H. P., & Ron, D. (2000). Coupling of stress in the ER to activation of JNK protein kinases by transmembrane protein kinase IRE1. *Science*, *287*(5453), 664–666.
66. van de Wetering, M., Sancho, E., Verweij, C., de Lau, W., Oving, I., Hurlstone, A., … Clevers, H. (2002). The β-Catenin/TCF-4 complex imposes a crypt progenitor phenotype on colorectal cancer cells. *Cell*, *111*(2), 241–250.
67. van der Flier, L. G., & Clevers, H. (2009). Stem Cells, self-renewal, and differentiation in the intestinal epithelium. *Annual Review of Physiology*, *71*(1), 241–260.
68. Vlantis, K., Wullaert, A., Sasaki, Y., Schmidt-Supprian, M., Rajewsky, K., Roskams, T., & Pasparakis, M. (2011). Constitutive IKK2 activation in

intestinal epithelial cells induces intestinal tumors in mice. *Journal of Clinical Investigation*, *121*(7), 2781–2793.
69. Vogelstein, B., Fearon, E. R., Hamilton, S. R., Kern, S. E., Preisinger, A. C., Leppert, M., … Bos, J. L. (1988). Genetic alterations during colorectal-tumor development. *New England Journal of Medicine*, *319*(9), 525–532.
70. Wang, M., & Kaufman, R. J. (2014). The impact of the endoplasmic reticulum protein-folding environment on cancer development. *Nature Reviews Cancer*, *14*(9), 581–597.
71. Wang, M., & Kaufman, R. J. (2016). Protein misfolding in the endoplasmic reticulum as a conduit to human disease. *Nature*, *529*(7586), 326–335.
72. Wang, Z., Gerstein, M., & Snyder, M. (2009). RNA-Seq: a revolutionary tool for transcriptomics. *Nature Reviews. Genetics*, *10*(1), 57–63.
73. Yoshida, H., Matsui, T., Yamamoto, A., Okada, T., & Mori, K. (2001). XBP1 mRNA is induced by ATF6 and spliced by IRE1 in response to ER stress to produce a highly active transcription factor. *Cell*, *107*(7), 881–891.
74. Zauber, A. G., Winawer, S. J., O'Brien, M. J., Lansdorp-Vogelaar, I., van Ballegooijen, M., Hankey, B. F., … Waye, J. D. (2012). Colonoscopic polypectomy and long-term prevention of colorectal-cancer deaths. *The New England Journal of Medicine*, *366*(8), 687–696.
75. Zhao, L. A dissertation submitted to the faculty of the graduate school of the University of Minnesota, 251.
76. Zhao, X., May, A., Lou, E., & Subramanian, S. (2018). Genotypic and phenotypic signatures to predict immune checkpoint blockade therapy response in patients with colorectal cancer. *Translational Research*, *0*(0).